Federal Reserve Bank of Boston®

Supervisory Research and Analysis Unit

Working Paper | SRA 24-02 | April 25, 2024

Scenario-based Quantile Connectedness of the U.S. Interbank Liquidity Risk Network

Tomohiro Ando, Jushan Bai, Lina Lu and Cindy M. Vojtech

Public Service That Makes a Difference®

bostonfed.org

Supervisory Research and Analysis (SRA) Working Papers present economic, financial and policy-related research conducted by staff in the Federal Reserve Bank of Boston's Supervisory Research and Analysis Unit. SRA Working Papers can be downloaded without charge at:
http://www.bostonfed.org/publications/sra/

Scenario-based Quantile Connectedness of the U.S. Interbank Liquidity Risk Network [1]

Tomohiro Ando[2] Jushan Bai[3] Lina Lu[4] and Cindy M. Vojtech[5]

April 18, 2024

Abstract

We characterize the U.S. interbank liquidity risk network based on a supervisory dataset, using a scenario-based quantile network connectedness approach. In terms of methodology, we consider a quantile vector autoregressive model with unobserved heterogeneity and propose a Bayesian nuclear norm estimation method. A common factor structure is employed to deal with unobserved heterogeneity that may exhibit endogeneity within the network. Then we develop a scenario-based quantile network connectedness framework by accommodating various economic scenarios, through a scenario-based moving average expression of the model where forecast error variance decomposition under a future pre-specified scenario is derived. The methodology is used to study the quantile-dependent liquidity risk network among large U.S. bank holding companies. The estimated quantile liquidity risk network connectedness measures could be useful for bank supervision and financial stability monitoring by providing leading indicators of the system-wide liquidity risk connectedness not only at the median but also at the tails or even under a pre-specified scenario. The measures also help identify systemically important banks and vulnerable banks in the liquidity risk transmission of the U.S. banking system.

JEL Classification: **C11, C31, C32, C33, C58, G21, G28**.

Keywords: Nuclear norm; Bayesian analysis; Scenario-based quantile connectedness; Bank supervision; Financial stability.

[1] We would like to thank a co-editor, an associate editor, and two anonymous referees for their insightful comments that greatly improved our paper. We are also grateful for helpful comments from Celso Brunetti, Ricardo Correa, Thibaut Duprey, Christopher Finger, Erik Heitfield, Ruben Hipp, Matthew Pritsker, and conference participants at the 2022 NBER-NSF Time Series Conference, the 2021 Bank of Canada, Federal Reserve Board, and Bank of Italy joint conference on "Non-traditional Data, Machine Learning and Natural Language Processing in Macroeconomics," and seminar participants at the Federal Reserve Board and University of Connecticut. A part of this work was completed when Tomohiro Ando was visiting Monash University. Tomohiro Ando would like to thank their generous supports during the visit. The views expressed in this paper are those of the authors and do not necessarily reflect the views of the Federal Reserve Bank of Boston or the Federal Reserve System. We also thank Antony Jippov, Stephen Shannon, Krish Sharma, and Xiyu Wang for their excellent research assistance. All remaining errors are ours.

[2] Melbourne Business School, University of Melbourne, T.Ando@mbs.edu.

[3] Department of Economics, Columbia University, jb3064@columbia.edu.

[4] Supervisory Research and Analysis Unit, Federal Reserve Bank of Boston, Lina.Lu@bos.frb.org.

[5] Division of Financial Stability, Federal Reserve Board, cindy.m.vojtech@frb.gov.

1 Introduction

Understanding the connectedness of financial networks is central to the study of shocks transmission and systemic risk, providing useful information for both risk management and financial stability monitoring. There have been many studies applying a vector-autoregressive (VAR) model together with the variance decomposition approach to investigate the network connectedness for financial institutions or sovereigns (e.g., Diebold and Yilmaz (2014); Alter and Beyer (2014); Diebold and Yilmaz (2015); Demirer et al. (2018); Hale and Lopez (2019); Miao et al. (2020); and Ando et al. (2022b)). However, most of the existing studies focus on financial assets or credit spread connectedness (e.g., stock and bond returns or return volatilities) rather than the liquidity risk network. Analyzing the interbank liquidity risk network allows us to better understand how banks liquidity risks are connected to each other and to identify systemically important banks or vulnerable banks, that could be useful for bank supervision and financial stability monitoring.

In addition, most studies examine network connectedness at the conditional mean instead of quantiles by assuming VAR coefficients are constant regardless of quantiles. The underlying assumption for the conditional mean analysis is that "large shocks propagate in the same way as smaller shocks" in forecast error variance decomposition. If the topology of a financial network changes with the size of the shock that affects the system, the results from a conventional mean model may lead to biased results (e.g., Ando et al. (2022b)). There is some work that analyzes quantile-dependent network connectedness, but they focus on the fixed-quantile case where the quantile point is fixed and the same in both dimensions, cross-sectional (e.g., cross individual institutions or banks), and over time (e.g., throughout the forecast horizon) (Ando et al. (2022b)).

Studying scenario-based quantile network connectedness where the quantile point (or the size of the shock) in a pre-specified future economic scenario could vary both cross-sectionally and throughout the forecast horizon, brings more flexibility to the implementation of the network analysis. Moreover, the existing literature concentrates on the variance decomposition based on idiosyncratic shocks rather than common shocks which could also be an important shock source for network connectedness. Furthermore, the previous studies (e.g., Cecchetti and Li (2008); Ando et al. (2022b)) study quantile network analysis under a fixed-quantile by using a model for the chosen quantile point. Different from these papers, we consider a scenario-based quantile network which needs the information from the entire conditional distribution rather than a model for a chosen quantile point. We propose a new method to extract the necessary information

from the entire conditional distribution for our network analysis. To our knowledge, there is no available method on measuring scenario-based quantile network connectedness and taking into account common shocks. There is also no existing empirical analysis on the quantile-dependent U.S. interbank liquidity risk network based on the variance decomposition. The challenge is mainly due to the non-straightforward task of preparing such a bank-level liquidity database, as well as access to a method that estimates the scenario-based quantile network connectedness by taking into account the endogeneity within the network.

Our paper attempts to fill this gap by first developing a methodology to compute scenario-based quantile network connectedness not only based on idiosyncratic shocks but also common shocks, using a quantile vector autoregressive (QVAR) model. Our model can be viewed as an extension of quantile vector autoregressive model without common shocks (Koenker and Xiao (2006), Schüler (2014)). For a traditional framework for quantile regression, we refer to Koenker and Bassett (1978). Then the proposed method is applied to empirically analyze the U.S. interbank liquidity risk network among large U.S. bank holding companies based on a supervisory dataset.

Specifically, for the methodology, we consider a QVAR model with unobserved heterogeneity (captured by a common factor structure) and propose a new Bayesian nuclear norm estimation approach. In terms of model estimation, we propose a new Bayesian Markov chain Monte Carlo (MCMC) approach to implement the nuclear norm estimation for QVAR with a common factor structure. We show that all these models can be estimated based on Gibbs sampling without relying on the Metropolis-Hastings approach. This implies that our Bayesian estimation approach enjoys the benefit of Gibbs sampling, including 100% acceptance rate of MCMC sampling and no need to prepare a proposal density. Similar to the existing frequentist nuclear norm estimation, our method does not require determining the number of common factors. Without specifying the number of common factors, Bayesian credible intervals for slope coefficients can be obtained. Moreover, Monte Carlo simulations show that the proposed Bayesian approach performs well in finite samples, especially compared to the frequentist nuclear norm estimation.

Then we develop a novel scenario-based quantile network connectedness framework by accommodating various economic scenarios, through a scenario-based moving average expression of QVAR which is established in Theorem 1. This general expression sheds light on the flexibility and importance of our QVAR framework because we are able to derive forecast error variance under a pre-specified future economic scenario as shown in Theorem 1. We then generalize the forecast error variance decomposition approach developed in Diebold and Yilmaz (2014) by dealing with the uncertainty associated with parameter estimation and model selection. A

special case of the scenario-based quantile network connectedness is the fixed-quantile network connectedness. Various network connectedness measures are considered: system-wide connectedness, pairwise directional connectedness, and total directional connectedness (connectedness between one bank and other banks). We further propose three different ways to analyze the network connectedness based on different sources of the shocks considered in the variance decomposition: (1) idiosyncratic shocks, (2) common shocks, and (3) combined shocks (combining idiosyncratic shocks and common shocks).

To support our novel Bayesian estimation procedure, we investigate the asymptotic behaviour of the posterior distribution for our QVAR model. There are many studies that investigate the posterior consistency for high-dimensional linear regression models for the analysis of cross sectional data (Ghoshal (1999); Bontemps (2010); Armagan et al. (2013); Sparks et al. (2015)). Recently, Ghosh et al. (2019) studies the posterior consistency for the high-dimensional "mean" vector autoregressive (VAR) model with Gaussian idiosyncratic errors when the dimension of individual units grows with the length of time series. However, little is known regarding the asymptotic properties of the posterior distribution for our QVAR model. There are several crucial differences between the high-dimensional "mean" VAR models and our QVAR models. More specifically, in contrast to the high-dimensional "mean" VAR model, the following additional features of our Bayesian QVAR needs to be taken care of when we establish the posterior consistency: the presence of the unobservable common factor structure, non-smoothness of the quantile loss function, nonlinearity of the quantile loss function in terms of parameters, and the Gaussian assumption is not imposed on the idiosyncratic error. These features make the theoretical analysis of our QVAR model challenging, but we were able to solve it and have provided theoretical analysis in the paper.

Regarding the empirical analysis, we use banks' liquidity coverage ratios (LCR) constructed from the supervisory FR 2052a Complex Institution Liquidity Monitoring Report data (more details are provided in Section 2). We evaluate the interbank liquidity risk network by implementing both the baseline fixed-quantile connectedness approach and the scenario-based quantile connectedness approach. In addition, we investigate the connectedness measures based on different types of shocks (idiosyncratic shocks, common shocks, or combined shocks).[6] In the

[6]In our interbank liquidity application, one example for idiosyncratic shock could be a customer loan from bank A. In order to meet that cash outlay, bank A could use cash, sell high-quality liquid assets (HQLA), or raise deposits; all of these options lower bank A's LCR. In managing LCR, bank A will likely try to offset the effect through several options: make transactions in the interbank market (reserves), make securities transactions, or compete for deposits. Both the actions to meet the initial liquidity shock (the loan) and the offsetting actions can affect other banks' LCR. One example of a common shock could be the COVID-19 shock, as it could impact one bank's LCR in the first place and then spill over to affect other banks through the interbank linkages.

fixed-quantile analysis, we study the network connectedness for various quantile points including both tails and median, mainly focusing on the pre- and during- COVID-19 periods. We find the liquidity risk network varies across quantiles and has changed substantially during COVID-19 pandemic relative to the pre-pandemic period; and it also changes according to the different source of the shocks used in the variance decomposition. In the scenario-based quantile analysis, we consider the Repo crisis during September 2019 and pre-specify the future economic scenario in the model based on the actual market movement during the Repo crisis. Our results indicate interesting connectedness patterns across different types of banks. We also look into the dynamic evolution of the quantile liquidity risk network by using a rolling window estimation.

From the perspective of bank supervision and financial stability monitoring, our approach of analyzing the U.S. interbank liquidity risk network provides empirical connectedness measures that would be useful for monitoring the banking system. In particular, our network measures help describe the strength of system-wide connectedness, and how one bank's liquidity risk affects another bank. The measures also show which banks are systemically important and which banks are vulnerable. Our network analysis is scenario-based and quantile-dependent, allowing us to investigate how the network changes across quantiles, especially between the median and the tails, and how the network behaves during a pre-specified scenario. In addition, the supervisory FR 2052a data used in our empirical analysis has not been extensively used in published liquidity papers. For instance, Ihrig et al. (2019) analyze how banks manage the composition of High-Quality Liquid Assets (HQLA) by looking at trends in the components and component volatility.[7] To the best of our knowledge, this paper is the first empirical study using this data to investigate the U.S. interbank liquidity risk network, providing network connectedness measures that could be useful for monitoring the banking system.

In the literature of nuclear norm estimation in statistics and econometrics, there have been many papers using it to estimate low rank matrices; see Koltchinskii et al. (2011), Negahban and Wainwright (2011), Negahban et al. (2012), Rohde and Tsybakov (2011), Chernozhukov et al. (2018), Fan et al. (2019), Moon and Weidner (2019), Miao et al. (2020), among others. All the preceding studies are implementing the nuclear norm technique under the frequentist estimation framework. Ding et al. (2011) develop a MCMC procedure to implement the Bayesian nuclear norm estimation for linear panel models. However, research on nonlinear models under the Bayesian estimation framework is limited. One of the main reasons might be the high nonlinearity of the objective function in terms of parameters, which makes it challenging to develop

[7] This data has also been used in some studies on understanding Collateral Re-use in the U.S. financial system and its drivers. See Infante et al. (2018, 2020) and Infante and Saravay (2020).

a Bayesian MCMC procedure.

In summary, our contributions are as follows. First, we propose a Bayesian nuclear norm estimation procedure for a QVAR model with a common factor structure and provide asymptotic analysis of the estimators. The proposed approach does not require determining the number of common factors and has comparable advantage with the existing frequentist estimation method. Second, we develop scenario-based quantile network connectedness measures, where the underlying future economic scenario could be pre-specified. The proposed connectedness measures can vary depending on different sources of shocks: idiosyncratic shocks, common shocks, or combined shocks (combining idiosyncratic and common shocks). Then, we apply the proposed method to study the U.S. interbank liquidity risk network using a supervisory dataset. The estimated quantile connectedness measures of the liquidity risk network could be useful for bank supervision and financial stability monitoring by providing leading indicators of the system-wide liquidity risk connectedness not only at the median but also at the tails or even under a specified scenario. The measures can also identify systemically important banks and vulnerable banks in the liquidity risk transmission.

The paper is organized as follows. Section 2 describes the data used in our empirical analysis. Section 3 introduces the model, estimation method, and scenario-based quantile network connectedness measures. Asymptotic analysis of the proposed estimator is provided in Section 4. In Section 5, the proposed method is applied to study the U.S. interbank liquidity risk network using a supervisory data set. Section 6 concludes.

2 Data

Bank supervision and liquidity monitoring play critical roles in maintaining the safety and soundness of the U.S. banking and financial system. For liquidity regulation, one key liquidity requirement, and the focus of this paper, is the LCR. LCR is defined as the ratio of HQLA over estimated 30-day net cash outflows, defined in Part 249 of the Code of Federal Regulations. LCR represents banks' ability to use highly liquid assets to meet the demand for cash over the short term. As per the applicable liquidity regulations, the largest U.S. domestic bank holding companies and intermediate holding companies of foreign banking organizations are expected to maintain an LCR above 100 percent daily. The implementation of the rule changed bank operations. Ihrig et al. (2019) show how bank holding companies significantly changed their balance sheets to comply with the rule. Rezende et al. (2021) show that the rule affected bank participation in monetary policy operations.

Liquidity data for the empirical exercise come from the FR 2052a data, collected from Com-

plex Institution Liquidity Monitoring Reports. The twelve domestic and foreign global systemically important banks (GSIBs) are required to report this information for each business day. Table 1 lists the twelve GSIBs and some summary financial data from the publicly available FR Y-9C data. The twelve banks are very different in terms of size and operations. The FR 2052a data contain detailed information on assets and liabilities that allow for the calculation of LCR on a daily basis.[8] For example, the data contain details for proper classification for outflow and inflow categories and are segmented by maturity date. These data are confidential and are not published. Sample data begin in January 2017 to avoid when banks first began to comply with the form where outliers suggest reporting errors. Because the daily LCR for the four foreign GSIBs are available since 4/24/2017 which is later compared to the eight U.S. GSIBs, we base our empirical analysis on the balanced panel from 4/24/2017 to 12/11/2020, for all the twelve banks. The pre-pandemic period is defined as 4/24/2017 - 12/31/2019, and the pandemic period is defined as 1/1/2020 - 12/11/2020.

3 Bayesian quantile connectedness of financial networks

In this section, we propose a new Bayesian framework for estimating QVAR model at a given quantile $\tau \in (0,1)$, to study the U.S. interbank liquidity risk network across quantiles using a non-publicly available supervisory liquidity dataset. We then develop a novel approach for the h-step-ahead forecast error variance decomposition and the associated scenario-based quantile connectedness measures. Specifically, we first consider a model for the entire conditional distribution rather than a model for a chosen quantile point. Then we obtain a moving-average representation for the model, based on that we compute the interconnectedness measures.

3.1 Quantile VAR with unobserved heterogeneity

For bank i at date t, suppose that the LCR, y_{it}, is observed for $t = 1, \ldots, T$, $i = 1, ..., N$. To capture the dynamics of the financial system, we consider the following quantile function for QVAR model with unobserved heterogeneity:

$$Q_{y_{it}}(\tau|\mathcal{F}_{t-1}) \equiv \sum_{h=1}^{p}\sum_{j=1}^{N} b_{ijh,\tau} y_{j,t-h} + z_{it,\tau} + G^{-1}_{e_{it}}(\tau), \tag{1}$$

where $\mathcal{F}_{t-1}$ denotes the information set available at time $t-1$, p is the lag of QVAR model, z_{it} is unobserved heterogeneity, e_{it} is the error term and $G^{-1}_{e_{it}}(\tau)$ is the τ-th quantile point of e_{it}

[8] More details about the form and reporting requirements can be found here https://www.federalreserve.gov/apps/reportforms/reportdetail.aspx?os5ofIRJDa8v/jn8ki6pKsdTYKX//BgQCZqE1VQAsoOjk00cVxyqN7JP7xdjdUN9.

with $G_{e_{it}}(\cdot)$ being the cumulative distribution function of e_{it}. We assume that e_{it} is identically distributed over t while its distribution may vary over i. The quantile function (1) can be derived from the following data generating process:

$$y_{it,u_{it}} = \sum_{h=1}^{p}\sum_{j=1}^{N} b_{ijh,u_{it}} y_{j,t-h} + z_{it,u_{it}} + e_{it,u_{it}}, \tag{2}$$

provided that the right hand side is an increasing function of u_{it}, where u_{it} follows the uniform distribution $U[0,1]$ and determines the quantile point of realization. This underlying model can be expressed in a vector form

$$\begin{bmatrix} y_{1t,u_{1t}} \\ \vdots \\ y_{Nt,u_{Nt}} \end{bmatrix} = \begin{bmatrix} \boldsymbol{b}'_{11,u_{1t}} \\ \vdots \\ \boldsymbol{b}'_{N1,u_{Nt}} \end{bmatrix} \begin{bmatrix} y_{1,t-1} \\ \vdots \\ y_{N,t-1} \end{bmatrix} + \cdots + \begin{bmatrix} \boldsymbol{b}'_{1p,u_{1t}} \\ \vdots \\ \boldsymbol{b}'_{Np,u_{Nt}} \end{bmatrix} \begin{bmatrix} y_{1,t-p} \\ \vdots \\ y_{N,t-p} \end{bmatrix} + \begin{bmatrix} z_{1t,u_{1t}} \\ \vdots \\ z_{Nt,u_{Nt}} \end{bmatrix} + \begin{bmatrix} e_{1t,u_{1t}} \\ \vdots \\ e_{Nt,u_{Nt}} \end{bmatrix},$$

where $\boldsymbol{b}_{ih,u_{it}} = (b_{i1h,u_{it}}, ..., b_{iNh,u_{it}})'$ is an $N \times 1$ vector representing the h-th lag coefficients. Unlike the traditional VAR, the QVAR coefficients vary over the quantiles. Also, the unobserved heterogeneity components are present. In the next section, we develop a new Bayesian procedure for estimating the QVAR coefficients by capturing the unobserved heterogeneity.

3.2 Bayesian nuclear norm estimation

In this section, we develop a new estimation procedure by introducing a Bayesian nuclear norm approach. Let τ be a specific quantile point. It is natural to consider the following objective function for estimating the parameters in (1):

$$\Pi_\tau(B_\tau, Z_\tau) = \frac{1}{NT}\sum_{i=1}^{N}\sum_{t=1}^{T} \rho_\tau(y_{it} - \boldsymbol{x}'_{it}\boldsymbol{b}_{i,\tau} - z_{it,\tau}), \tag{3}$$

where $\rho_\tau(u) = u(\tau - 1(u < 0))$ is the quantile loss function with $1(\cdot)$ being the indicator function that takes value one if the expression in the brackets are satisfied, and zero otherwise, y_{it} is realized observation, $\boldsymbol{x}_{it} \equiv (1, \boldsymbol{y}'_{t-1}, ..., \boldsymbol{y}'_{t-p})'$, $\boldsymbol{y}_t = (y_{1t}, y_{2t}, \cdots, y_{Nt})'$ is an $N \times 1$ vector with each element y_{it} representing the LCR for bank i at date t, $\boldsymbol{b}_{i,\tau} \equiv (b_{i0,\tau}, \boldsymbol{b}'_{i1,\tau}, ..., \boldsymbol{b}'_{ip,\tau})'$ with $b_{i0,\tau} = G^{-1}_{e_i}(\tau)$, and $\boldsymbol{b}_{ih,\tau} = (b_{i1h,\tau}, ..., b_{iNh,\tau})'$ being an $N \times 1$ vector representing the hth lag QVAR coefficients. Notice that the τ-th quantile of the idiosyncratic error $G^{-1}_{e_i}(\tau)$ is absorbed by the term $\boldsymbol{x}'_{it}\boldsymbol{b}_{i,\tau}$.

The direct minimization (3) causes numerical issues. This is because the number of parameters in the model is larger than the number of data points. Some regularizations are

necessary. Following the common factor literature (Bai and Ng (2019)), we use the nuclear norm penalization. All unknown parameters in the model (1) are jointly estimated by, for some $0 < r < \min\{T, N\}$,

$$\text{argmin}_{B_\tau, Z_\tau:\text{rank}(Z_\tau)\leq r} \left[\Pi_\tau(B_\tau, Z_\tau) + \gamma\|Z_\tau\|_*\right], \tag{4}$$

where Z_τ is a $T \times N$ matrix with (t,i)-th element being $z_{it,\tau}$, γ is the regularization parameter and $\|\cdot\|_*$ is the nuclear norm. Note that by assuming $Z_\tau = (z_{it,\tau})$ is a lower rank matrix with rank r, then

$$\|Z_\tau\|_* = \min_{F_\tau, \Lambda_\tau: Z_\tau = F_\tau\Lambda_\tau} \frac{1}{2}(\|F_\tau\|_F^2 + \|\Lambda_\tau\|_F^2), \tag{5}$$

where $\|\cdot\|_F$ is Frobenius norm, $F_\tau = (\boldsymbol{f}_{1,\tau}, ..., \boldsymbol{f}_{T,\tau})'$ and $\Lambda_\tau = (\boldsymbol{\lambda}_{1,\tau}, ..., \boldsymbol{\lambda}_{N,\tau})$ are $T \times r$ and $r \times N$ dimensional matrices (e.g., Hastie et al. (2015) and Bai and Ng (2019)). The structure $Z_\tau = F_\tau\Lambda_\tau$ can be linked to the factor analysis literature. Thus, the term $z_{it,\tau} = \boldsymbol{f}_{t,\tau}'\boldsymbol{\lambda}_{i,\tau} = \sum_{k=1}^r f_{tk,\tau}'\lambda_{ik,\tau}$ is the common factor structure capturing unobserved heterogeneity, where $\boldsymbol{f}_{t,\tau} = (f_{t1,\tau}, ..., f_{tr,\tau})'$ denotes the common factors at date t and $\boldsymbol{\lambda}_{i,\tau} = (\lambda_{i1,\tau}, ..., \lambda_{ir,\tau})'$ denotes the factor loadings vector. We can rewrite (1) as

$$Q_{y_{it}}(\tau|\mathcal{F}_{t-1}) \equiv \sum_{h=1}^{p}\sum_{j=1}^{N} b_{ijh,\tau}y_{j,t-h} + \sum_{k=1}^{r} f_{tk,\tau}\lambda_{ik,\tau} + G_{e_{it}}^{-1}(\tau), \tag{6}$$

where the unobserved heterogeneity z_{it} is expressed as a common factor structure. Note that the number of free parameters in terms of heterogeneity z_{it} in (1) is $N \times T$, while that in (6) is $(N+T)r$. Therefore, the number of parameters are reduced significantly. The minimization problem (4) is equivalent to

$$\text{argmin}_{B_\tau, F_\tau, \Lambda_\tau} \left[\Pi_\tau(B_\tau, F_\tau, \Lambda_\tau) + \kappa_\tau\|F_\tau\|_F^2 + \kappa_\tau\|\Lambda_\tau\|_F^2\right], \tag{7}$$

where $\Pi_\tau(B_\tau, F_\tau, \Lambda_\tau) \equiv \frac{1}{NT}\sum_{i=1}^N\sum_{t=1}^T \rho_\tau(y_{it} - \boldsymbol{x}_{it}'\boldsymbol{b}_{i,\tau} - \boldsymbol{f}_{t,\tau}'\boldsymbol{\lambda}_{i,\tau})$ and κ is a regularization parameter. A large value of regularization parameter κ_τ forces less flexibility of F_τ and Λ_τ in the sense that their norms $\|F_\tau\|_F^2$ and $\|\Lambda_\tau\|_F^2$ get closer to zero. On the other hand, a small value of κ_τ allows F_τ and Λ_τ place more emphasis on the quantile loss part $\Pi_\tau(B_\tau, F_\tau, \Lambda_\tau)$. In other words, the regularization term on F_τ and Λ_τ becomes nearly negligible when the regularization parameter κ_τ is extremely close to zero. Because we further put a prior on κ_τ, our Bayesian estimation procedure takes a balance between the quantile loss and the regularization terms on F_τ and Λ_τ through MCMC Gibbs sampling.

We use $\Pi_\tau(B_\tau, F_\tau, \Lambda_\tau)$ in (7) as our objective function for Bayesian analysis. In the Bayesian framework, the pseudo-likelihood function is

$$L(Y|B_\tau, F_\tau, \Lambda_\tau) \propto \exp\left(-\Pi_\tau(B_\tau, F_\tau, \Lambda_\tau)\right).$$

For the data-augmentation approach, we need to specify the prior distribution of the parameters. For ease of computation, we assume that the priors of the factors, factor loadings, coefficients and parameter κ are mutually independent, i.e., prior distribution $\pi(B_\tau, F_\tau, \Lambda_\tau, \kappa_\tau) = \pi(B_\tau)\pi(F_\tau)\pi(\Lambda_\tau)\pi(\kappa_\tau)$. As in (7), we can view that the prior distributions for F and Λ are corresponding to $\pi(F_\tau) \propto \exp(-\kappa_\tau \|F_\tau\|_F^2)$ and $\pi(\Lambda_\tau) \propto \exp(-\kappa_\tau \|\Lambda_\tau\|_F^2)$. It can be seen that these are the kernel of multivariate normal distribution. We use a diffuse prior on B_τ such that $\pi(B_\tau) \propto$ constant and place the class of gamma prior on κ_τ of the form $\pi(\kappa_\tau) = \frac{\delta^a}{\Gamma(a)}(\kappa_\tau)^{a-1}\exp(-\delta\kappa_\tau)$ with $a > 0$ and $\delta > 0$. Then, the posterior density will be

$$\pi(B_\tau, F_\tau, \Lambda_\tau, \kappa_\tau | Y) \propto L(Y|B_\tau, F_\tau, \Lambda_\tau)\pi(B_\tau)\pi(\Lambda_\tau)\pi(F_\tau)\pi(\kappa_\tau).$$

This expression does not provide analytical posterior density forms, but we can estimate the posterior density through the MCMC approach. Appendix A provides more details on the prior and posterior analysis of parameters. MCMC computation is implemented solely based on Gibbs sampling without relying on Metropolis-Hesting sampling, thanks to the data augmentation procedure (Ando and Bai (2020), Polson and Scott (2013)). Thus, the generated samples are always accepted unlike Metropolis-Hesting sampling. Using a set of generated posterior samples for the parameters in (6), $\{B_\tau^{(a)}, F_\tau^{(a)}, \Lambda_\tau^{(a)}\}$ for $a = 1, ..., H$, we can calculate various quantities. Here H is the number of generated posterior samples. For example, plugging the a-th posterior sample $\{B_\tau^{(a)}, F_\tau^{(a)}, \Lambda_\tau^{(a)}\}$ into model (1), the τ-th quantile function for i-th unit becomes

$$Q_{y_{it}}(\tau|\mathcal{F}_{t-1})^{(a)} \equiv \sum_{h=1}^{p}\sum_{j=1}^{N} b_{ijh,\tau}^{(a)} y_{j,t-h} + \sum_{k=1}^{r} f_{tk,\tau}^{(a)} \lambda_{ik,\tau}^{(a)} + G_{e_{it}}^{-1}(\tau)^{(a)}, \tag{8}$$

for $a = 1, ..., H$. Appendix D conducts Monte Carlo simulations. It is shown that the proposed method captures the underlying structure well.

Remark 1 Our Bayesian approach does not require determining the number of common factors r. Without specifying the number of common factors, Bayesian credible intervals for any functions of QVAR parameters can be obtained automatically. Thus the parameter uncertainty, as well as the model selection uncertainty associated with selecting the number of common factors, are addressed automatically. Under the frequentist framework, there are several studies that employ the nuclear norm penalty to estimate the panel quantile regression with interactive fixed effects (Belloni et al. (2023); Moon and Weidner (2019); Feng (2023)). However, the previous studies mainly focus on the asymptotic property of their estimators under the nuclear norm penalty, and the question about theoretical study on the model selection still remains. Also, the frequentist approach selects one final model which corresponds to a best size of the nuclear norm

penalty, implying that the model selection uncertainty is ignored. In contrast, as an advantage of our Bayesian method, a set of posterior draws of κ_τ produces a set of nuclear norm penalties with different sizes and thus reflects different model specifications implicitly.

Remark 2 It is well known that the common factors and the loadings are not uniquely identified without imposing identification restrictions (see for example, Bai and Ng (2013)). Although the prior structures $\pi(F_\tau) \propto \exp(-\kappa_\tau \|F_\tau\|_F^2)$ and $\pi(\Lambda_\tau) \propto \exp(-\kappa_\tau \|\Lambda_\tau\|_F^2)$ do not contain the identification restrictions on F_τ and Λ_τ, we can impose conditions on the posterior samples to achieve a full identification. For example, we adopt the following identification conditions:

$$\frac{1}{T} F_\tau' F_\tau = I_r, \ \frac{1}{N} \Lambda_\tau' \Lambda_\tau = D_\tau, \tag{9}$$

where D_τ is a diagonal matrix whose diagonal elements are distinct. Recall that we have a set of posterior samples of the factor structure $\{F_\tau^{(a)}, \Lambda_\tau^{(a)}\}$ for $a = 1, ..., H$. Define $R_\tau^{(a)}$ to be the matrix consisting of the eigenvectors of the matrix $(\frac{1}{T} F_\tau^{(a)'} F_\tau^{(a)})^{1/2} (\frac{1}{N} \Lambda_\tau^{(a)'} \Lambda_\tau^{(a)}) (\frac{1}{T} F_\tau^{(a)'} F_\tau^{(a)})^{1/2}$. Then, the following rotation $\tilde{\boldsymbol{f}}_{t,\tau}^{(a)} = R_\tau^{(a)'} (\frac{1}{T} F_\tau^{(a)'} F_\tau^{(a)})^{-1/2} \boldsymbol{f}_{t,\tau}^{(a)}$ and $\tilde{\boldsymbol{\lambda}}_{i,\tau}^{(a)} = R_\tau^{(a)'} (\frac{1}{T} F_\tau^{(a)'} F_\tau^{(a)})^{1/2} \boldsymbol{\lambda}_{i,\tau}^{(a)}$ satisfy the identification conditions (9). These restrictions are also used by Ando and Bai (2015); Ando et al. (2022a); Song (2013) for example. Finally, we note that rotational indeterminacy does not affect the estimation of the other coefficients B_τ.

3.3 Scenario-based quantile connectedness

This section introduces the scenario-based quantile connectedness measure where the underlying future economic scenario could be arbitrarily specified. We define network connectedness measures based on different types of shocks: (1) idiosyncratic shocks, (2) common shocks, and (3) combined shocks (combining idiosyncratic and common shocks), by taking advantage of the common factor structure in the model.

Specifically, after estimating the model in (6), we compute our quantile connectedness measures by generalizing the forecast error variance decomposition approach developed in Diebold and Yilmaz (2014) from the conditional mean to quantiles. Traditionally, a concept of impulse response function used in the literature is defined as the difference between two different scenarios of $\boldsymbol{y}_{t+h,u_{t+h}}$ that are identical up to time $t-1$. One scenario assumes that between t and $t+h$ the system is hit only by a certain size of shock at time t. The other scenario, taken as the benchmark, assumes that the system is not hit by any shock between t and $t+h$. This traditional framework is designed to provide an answer to the question: "What is the effect of a certain size of shock on a system at time t on the state of the system at time $t+h$, given that

no other shocks occurs to the system during this time period?" As mentioned in Koop et al. (1996), this concept is more usefully applied to linear VAR models than to nonlinear models.

To address this disadvantage of traditional impulse response functions for nonlinear models, Koop et al. (1996) introduced a concept of the generalized impulse response function. This concept treats the future by using the expectation operator conditioned on only the history and/or shock. That is, the future shocks are averaged out. Thus, the response constructed is an average of what might happen given the present and the past. The natural baseline for the impulse response function is then defined as the conditional expectations, given only the history. This leaves the question of how to perturb the present to produce information on the dynamics of the system. Therefore, in this paper, we propose scenario-based connectedness measures where the shock at time t can be arbitrarily specified, as well as the future economic scenario throughout the forecast horizon.

In the following, we first introduce the scenario-based moving average expression of the QVAR model and then derive forecast error variance based on it. Let $\boldsymbol{\tau} = (\tau_1, ..., \tau_N)'$ be a focused quantile vector for a set of N individuals. We denote $\boldsymbol{u}_t = (u_{1t}, ..., u_{Nt})'$ as an N-dimensional vector of uniform $U(0,1)$ variables that determine the realization of $\boldsymbol{\tau}$ at time t. Recall that our model is

$$\begin{bmatrix} y_{1t,u_{1t}} \\ \vdots \\ y_{Nt,u_{Nt}} \end{bmatrix} = \begin{bmatrix} \boldsymbol{b}'_{11,u_{1t}} \\ \vdots \\ \boldsymbol{b}'_{N1,u_{Nt}} \end{bmatrix} \begin{bmatrix} y_{1,t-1,u_{1,t-1}} \\ \vdots \\ y_{N,t-1,u_{N,t-1}} \end{bmatrix} + \cdots + \begin{bmatrix} \boldsymbol{b}'_{1p,u_{1t}} \\ \vdots \\ \boldsymbol{b}'_{Np,u_{1N}} \end{bmatrix} \begin{bmatrix} y_{1,t-p,u_{1,t-p}} \\ \vdots \\ y_{N,t-p,u_{N,t-p}} \end{bmatrix} + \begin{bmatrix} \boldsymbol{f}'_{t,u_{1t}} \boldsymbol{\lambda}_{1,u_{1t}} \\ \vdots \\ \boldsymbol{f}'_{t,u_{Nt}} \boldsymbol{\lambda}_{N,u_{Nt}} \end{bmatrix} + \begin{bmatrix} e_{1t,u_{1t}} \\ \vdots \\ e_{Nt,u_{Nt}} \end{bmatrix},$$

or in a compact form,

$$\boldsymbol{y}_{t,u_t} = \sum_{k=1}^{p} B_{k,u_t} \boldsymbol{y}_{t-k,u_{t-k}} + \boldsymbol{z}_{t,u_t} + \boldsymbol{e}_{t,u_t}, \tag{10}$$

where $B_{k,u_t} = (\boldsymbol{b}_{1k,u_{1t}}, ..., \boldsymbol{b}_{Nk,u_{Nt}})'$, $\boldsymbol{z}_{t,u_t}$ is an N-dimensional vector with i-th element being $\boldsymbol{f}'_{t,u_{it}} \boldsymbol{\lambda}_{i,u_{it}}$, and $\boldsymbol{e}_{t,u_t}$ is an N-dimensional vector of idiosyncratic error terms with i-th element being $\boldsymbol{e}_{it,u_{it}}$. By assuming that the right hand side of (10) is an increasing function of $u_{it} \in (0,1)$, then the quantile function in (6) is implied by (10).

Remark 3 As we can see in (10), the factor loadings and common factors depend on (i,t) through u_{it}. Once u_{it} is fixed to be τ, the factor loadings become $\boldsymbol{\lambda}_{i,\tau}$ and will only depend on i. The same argument is true for the common factors as once u_{it} is fixed to be τ, the common

factor become $\boldsymbol{f}_{t,\tau}$ and will only depend on t.

Unlike the precedent established by Cecchetti and Li (2008) and Ando et al. (2022b) in the context of multivariate forecasting with dynamic quantile regressions, where the quantile index $\boldsymbol{\tau}$ is fixed across sectional (i.e., across individuals) and throughout the forecast horizon, our approach described below allows for the quantile index to vary through the forecast horizon as well as across individuals. To develop network statistics based on quantile forecasting error variance decomposition, the following theorem is useful. Before we develop the theorem, we introduce some notation. Let $\boldsymbol{\tau}_t = (\tau_{1,t}, ..., \tau_{N,t})'$ be an N-dimensional vector that specifies quantile points at time t with element $\tau_{i,t}$ presenting the specific quantile point for unit i. Define the following matrices:

$$\Psi_t(\boldsymbol{\tau}_t) \equiv \begin{bmatrix} B_{1,\boldsymbol{\tau}_t} & B_{2,\boldsymbol{\tau}_t} & \cdots & B_{p-1,\boldsymbol{\tau}_t} & B_{p,\boldsymbol{\tau}_t} \\ I & O & \cdots & O & O \\ O & I & \cdots & O & O \\ \vdots & \vdots & \ddots & \vdots & \vdots \\ O & O & \cdots & I & O \end{bmatrix},$$

$$\Gamma_{t,k}(\boldsymbol{\tau}_t, \boldsymbol{\tau}_{t-1}, ..., \boldsymbol{\tau}_{t-k}) \equiv \Psi_t \Psi_{t-1} \cdots \Psi_{t-k} = \begin{bmatrix} \Gamma_{11,tk} & \cdots & \Gamma_{1p,tk} \\ \vdots & \ddots & \vdots \\ \Gamma_{p1,tk} & \cdots & \Gamma_{pp,tk} \end{bmatrix}, \quad k = 1, ...$$

and $\Gamma_{t,k} = I$ for $k = 0$. Here $\Gamma_{ab,tk}$ denotes the (a, b)-th block element of $\Gamma_{t,k}$, and I is an $N \times N$ identity matrix. Note that, for notational simplicity, the dependency of quantile points $\boldsymbol{\tau}_t$, $\boldsymbol{\tau}_{t-1}$,..., is dropped in the matrix representation of $\Gamma_{t,k}$. Finally, we define

$$\Phi_{t,k} \equiv \Phi_{t,k}(\boldsymbol{\tau}_t, \boldsymbol{\tau}_{t-1}, ..., \boldsymbol{\tau}_{t-k}) \equiv \Gamma_{11,tk}(\boldsymbol{\tau}_t, \boldsymbol{\tau}_{t-1}, ..., \boldsymbol{\tau}_{t-k}), \tag{11}$$

which is the $(1, 1)$-th block element of $\Gamma_{t,k}(\boldsymbol{\tau}_t, \boldsymbol{\tau}_{t-1}, ..., \boldsymbol{\tau}_{t-k})$. Then we have the following theorem.

Theorem 1 *Quantile VAR model (10) has the following moving average expression:*

$$\boldsymbol{y}_{t,u_t} = \sum_{k=0}^{\infty} \Phi_{t,k}(\boldsymbol{u}_t, \boldsymbol{u}_{t-1}, ..., \boldsymbol{u}_{t-k}) \boldsymbol{z}_{t-k,u_{t-k}} + \sum_{k=0}^{\infty} \Phi_{t,k}(\boldsymbol{u}_t, \boldsymbol{u}_{t-1}, ..., \boldsymbol{u}_{t-k}) \boldsymbol{e}_{t-k,u_{t-k}}, \tag{12}$$

where $\Phi_{t,k}(\boldsymbol{u}_t, \boldsymbol{u}_{t-1}, ..., \boldsymbol{u}_{t-k})$ *is given in (11).*

Remark 4 We note that the expression (12) is quite general. It encompasses both stationary and non-stationary cases. There are several studies that investigated the stationarity of the high-dimensional "mean" VAR models, which implicitly assumes that VAR coefficients do not vary over quantiles (Basu and Michailidis (2015); Kock and Callot (2015); Miao et al. (2020)).

For non-stationarity VAR case, we refer to Phillips (1998). When the VAR coefficients do not vary across quantiles, the second term on the right hand side in (12) is stationary when the minimum and the maximum eigenvalues of covariance matrix of $\boldsymbol{e}_{t,u_t}$ are bounded away from zero and infinity, and $\boldsymbol{e}_{t,u_t}$ is serially uncorrelated (Miao et al. (2020)). In contrast, the VAR coefficients vary across quantiles in the moving average expression (12). Assumption E given in Section 4 below is a sufficient condition for the stationarity of the second term in (12). For the first term on the right hand side in (12), Assumption (E1) together with Assumption A and Assumption B given in Section 4 becomes a sufficient condition for the stationarity. Relaxing these to more general conditions is not the focus of this study.

Remark 5 Assume that the QVAR is stationary. If we assume that the quantile point is identical across individual units as well as throughout the entire time period, i.e., $\boldsymbol{\tau}_t = \boldsymbol{\tau} = (\tau, ..., \tau)'$ for all t, the expression (12) reduces to the Wold representation in Ando et al. (2022b): $\boldsymbol{y}_{t,\tau} = \sum_{k=0}^{\infty} \Phi_{k,\tau} \boldsymbol{e}_{t-k,\tau} + \sum_{k=0}^{\infty} \Phi_{k,\tau} \Lambda_\tau \boldsymbol{f}_{t-k,\tau}$, where the $N \times N$ coefficient matrices $\Phi_{j,\tau}$ satisfy the recursion $\Phi_{j,\tau} = B_{1,\tau}\Phi_{j-1,\tau} + B_{2,\tau}\Phi_{j-2,\tau} + \cdots + B_{p,\tau}\Phi_{j-p,\tau}$, with $\Phi_{0,\tau} = I$ and $\Phi_{j,\tau} = 0$ for $j < 0$. Here $B_{k,\tau} = (\boldsymbol{b}_{1k,\tau}, ..., \boldsymbol{b}_{Nk,\tau})'$ and $\Lambda = (\boldsymbol{\lambda}_{1,\tau}, ..., \boldsymbol{\lambda}_{N,\tau})'$. If we further assume that there are no unobserved heterogeneity components, and all regression coefficients do not vary across quantiles, we then obtain the traditional Wold representation of the VAR model.

From (12), we can see that the response $\boldsymbol{y}_{t,u_t}$ is driven by two components. One component is the idiosyncratic error, and the other is from the unobserved heterogeneity. Such a model specification allows us to analyze network connectedness not only based on the idiosyncratic component but also based on the unobserved heterogeneity. Similar to many studies in the literature of network connectedness analysis, we can investigate network connectedness based on the idiosyncratic component conditioning on the unobserved heterogeneity, to focus on the idiosyncratic contagion connectedness, which is the so-called idiosyncratic-component-based variance decomposition approach. See Diebold and Yilmaz (2014), Hale and Lopez (2019), Miao et al. (2020), and Ando et al. (2022b). Moreover, we can study the network connectedness based on the unobserved heterogeneity conditioning on the idiosyncratic component and even the overall connectedness based on both of them. Furthermore, we propose scenario-based quantile connectedness using a Bayesian approach, in order to accommodate various forecasting paths by allowing the quantile point varying through the forecast path and also across individual units.

Let h be a forecast horizon and $\boldsymbol{\tau}_t, ..., \boldsymbol{\tau}_{t+h}$ be a vector of quantile points that specify a future scenario. From Theorem 1, it follows that the forecasting errors of predicting $\boldsymbol{y}_{t+h,\boldsymbol{\tau}_{t+h}}$

conditional on the information $\mathcal{F}_{t-1}$ is given by

$$\boldsymbol{\varepsilon}_{t+h,\boldsymbol{\tau}_{t+h}} = \sum_{k=0}^{h} \Phi_{t+h,k}(\boldsymbol{\tau}_{t+h},...,\boldsymbol{\tau}_{t+h-k})\boldsymbol{z}_{t+h-k,\boldsymbol{\tau}_{t+h-k}} + \sum_{k=0}^{h} \Phi_{t+h,k}(\boldsymbol{\tau}_{t+h},...,\boldsymbol{\tau}_{t+h-k})\boldsymbol{e}_{t+h-k,\boldsymbol{\tau}_{t+h-k}},$$

where $\boldsymbol{\tau}_t$, $\boldsymbol{\tau}_{t+1}$,...,$\boldsymbol{\tau}_{t+h}$ is a path of the scenario. Following Diebold and Yilmaz (2014), we use the "generalization identification" approach to handle the identification challenge in the VAR model. The "generalization identification" framework allows us to produce forecast error variance decomposition invariant to order, while the traditional Cholesky decomposition depends on the ordering of the variables which is not easily determined. Before we introduce our new approach for measuring scenario-based quantile connectedness, the following property is useful.

Assume that the QVAR is stationary, and that $\boldsymbol{z}_{\boldsymbol{\tau}_t}$ and $\boldsymbol{e}_{\boldsymbol{\tau}_t}$ are uncorrelated over t. Under no serial correlation for both $\boldsymbol{z}_{\boldsymbol{\tau}_t}$ and $\boldsymbol{e}_{\boldsymbol{\tau}_t}$, the total forecast error variance matrix is:

$$\text{FEV}(\boldsymbol{\varepsilon}_{t+h,\boldsymbol{\tau}_{t+h}}|\boldsymbol{\tau}_t,\boldsymbol{\tau}_{t+1},...,\boldsymbol{\tau}_{t+h}) = \sum_{k=0}^{h} \Phi_{t+h,k}\boldsymbol{\Omega}_z\Phi'_{t+h,k} + \sum_{k=0}^{h} \Phi_{t+h,k}\boldsymbol{\Omega}_e\Phi'_{t+h,k}, \tag{13}$$

where $\Phi_{t+h,k}$ is defined in (11), $\boldsymbol{\Omega}_z$ is the variance matrix of $\boldsymbol{z}_{t,u_t}$, and $\boldsymbol{\Omega}_e$ is the variance matrix of $\boldsymbol{e}_{t,u_t}$. Note that FEV reflects the surprise of the path of future scenario $\boldsymbol{\tau}_t$, $\boldsymbol{\tau}_{t+1}$,...,$\boldsymbol{\tau}_{t+h}$ through $\Phi_{t+h,k}$.

Remark 6 While the total forecast error variance matrix (13) is derived under no serial correlation in both $\boldsymbol{z}_{t,u_t}$ and $\boldsymbol{e}_{t,u_t}$, we note that the outcome variable $\boldsymbol{y}_{t,u_t}$ follows a QVAR model which exhibits serial correlation.

In the following, we define our scenario-based quantile connectedness measures in three ways based on different types of shocks: (1) based on the idiosyncratic shocks component, (2) based on the unobserved heterogeneity (the common shocks component) and (3) based on the combined shocks (combining idiosyncratic shocks and common shocks).

3.3.1 Quantile connectedness based on idiosyncratic shocks

Many studies in the literature (Cecchetti and Li (2008), Ando et al. (2022b), and others) investigate quantile connectedness based on idiosyncratic shocks by employing the quantile based forecast error variance. However, in these studies, the quantile index is fixed throughout the forecast horizon. Our framework is distinct from these existing methods by the nature of our forecast error variance in (13), which allows the quantile index to change across the forecast horizon as well as across individual units.

We define our scenario-based quantile connectedness measures by starting with granular pairwise directional connectedness. Let $\tilde{C}^{e}_{i\leftarrow j,h,\boldsymbol{\tau}}$ denote the proportion of bank i's h-step-ahead

generalized forecast error variance due to idiosyncratic shocks from bank j, conditional on the future scenario $\boldsymbol{\tau} = (\boldsymbol{\tau}_t, ..., \boldsymbol{\tau}_{t+h})$ (alternatively, $\boldsymbol{\tau}_t \to \boldsymbol{\tau}_{t+1} \to \cdots \to \boldsymbol{\tau}_{t+h}$), defined as

$$\tilde{C}^e_{i\leftarrow j,h,\boldsymbol{\tau}} = \frac{\sum_{k=0}^{h-1} \hat{\omega}_{jj,e}^{-1} \left(l_i' \hat{\Phi}_k \hat{\boldsymbol{\Omega}}_e l_j\right)^2}{\sum_{k=0}^{h-1} \left(l_i' \hat{\Phi}_k \hat{\boldsymbol{\Omega}}_e \hat{\Phi}_k' l_i\right)}, \qquad i = 1, 2, \cdots, N;\ j = 1, 2, \cdots, N, \tag{14}$$

where $\hat{\boldsymbol{\Omega}}_e$ is the estimated covariance matrix of the error vector $\boldsymbol{e}_{\boldsymbol{\tau}_{t+h-k}}$, $\hat{\omega}_{jj,e}$ is the jth diagonal element of $\hat{\boldsymbol{\Omega}}_e$, and l_i is an $N \times 1$ selection vector with its ith entry being one and zero otherwise. In our application of liquidity risk network, $\tilde{C}^e_{i\leftarrow j,h,\boldsymbol{\tau}}$ represents how much of bank i's future liquidity uncertainty (at horizon h) is due to idiosyncratic liquidity shocks arising with bank j conditioning on the specific future scenario $\boldsymbol{\tau}$. Note that the diagonal element $\tilde{C}^e_{i\leftarrow i,h,\boldsymbol{\tau}}$ measures the self-link, how much of bank i's future liquidity uncertainty (at horizon h) is due to its own idiosyncratic liquidity shocks based on the scenario $\boldsymbol{\tau}$.

Under the "generalization identification" framework, the variance shares do not necessarily sum up to one, in other words, generally $\sum_{j=1}^N \tilde{C}^e_{i\leftarrow j,h,\boldsymbol{\tau}} \neq 1$. Thus we row-normalize the matrix $(\tilde{C}^e_{i\leftarrow j,h,\boldsymbol{\tau}})$, denoted as $(C^e_{i\leftarrow j,h,\boldsymbol{\tau}})$ with $C^e_{i\leftarrow j,h,\boldsymbol{\tau}} = \frac{\tilde{C}^e_{i\leftarrow j,h,\boldsymbol{\tau}}}{\sum_{j=1}^N \tilde{C}^e_{i\leftarrow j,h,\boldsymbol{\tau}}}$. From now on, we base our analysis on the row-normalized pairwise connectedness.

Next, we compute total directional connectedness including "To", "From," and "Net" measures. Specifically, the "To" measure represents the total directional connectedness from bank i *to others* defined as

$$C^e_{\bullet\leftarrow i,h,\boldsymbol{\tau}} = \sum_{j=1, j\neq i}^{N} C^e_{j\leftarrow i,h,\boldsymbol{\tau}}. \tag{15}$$

Similarly, the "From" measure represents the total directional connectedness *from others* to bank i, defined as

$$C^e_{i\leftarrow \bullet,h,\boldsymbol{\tau}} = \sum_{j=1, j\neq i}^{N} C^e_{i\leftarrow j,h,\boldsymbol{\tau}}. \tag{16}$$

By definition, the "From" measure is always equal to or smaller than one, while the "To" measure could be larger than one. Based on "To" and "From," we define "Net" as (To - From), by subtracting "From" from "To," representing the net connectedness between bank i and others.

In our interbank liquidity network, "To" represents the system impact of a bank's liquidity shock on other banks' liquidity, i.e., a bank's systemic importance. On the other hand, "From" represents a bank's vulnerability, specifically how would a bank's liquidity be affected by other banks' liquidity shocks.

Finally, we compute total connectedness, also known as system-wide connectedness, defined as

$$C^{e}_{h,\boldsymbol{\tau}} = \frac{1}{N} \sum_{i,j=1,i\neq j}^{N} C^{e}_{i\leftarrow j,h,\boldsymbol{\tau}}. \tag{17}$$

These measures include both disaggregate and aggregate level information on the topology of the network, that could be useful for both risk management and bank supervision. Risk managers might be more interested in the disaggregated pairwise directional connectedness, while regulators might be more concerned with the aggregate level total connectedness as well as the total directional connectedness where "To" measures each bank's systemic importance and "From" measures each bank's vulnerability.

3.3.2 Quantile connectedness based on common shocks

We define quantile connectedness based on common shocks (through the unobserved heterogeneity), in a similar way as the quantile connectedness based on the idiosyncratic component in the previous section. Let $\tilde{C}^{z}_{i\leftarrow j,h,\boldsymbol{\tau}}$ denotes the proportion of bank i's h-step-ahead generalized forecast error variance due to shocks to the unobserved heterogeneity of bank j, conditional on the future scenario $\boldsymbol{\tau} = (\boldsymbol{\tau}_t, ..., \boldsymbol{\tau}_{t+h})$ (alternatively, $\boldsymbol{\tau}_t \to \boldsymbol{\tau}_{t+1} \to \cdots \to \boldsymbol{\tau}_{t+h}$), defined as

$$\tilde{C}^{z}_{i\leftarrow j,h,\boldsymbol{\tau}} = \frac{\sum_{k=0}^{h-1} \hat{\omega}^{-1}_{jj,z} \left(l_i' \hat{\Phi}_k \hat{\boldsymbol{\Omega}}_z l_j\right)^2}{\sum_{k=0}^{h-1} \left(l_i' \hat{\Phi}_k \hat{\boldsymbol{\Omega}}_z \hat{\Phi}_k' l_i\right)}, \qquad i = 1, 2, \cdots, N;\ j = 1, 2, \cdots, N, \tag{18}$$

where $\hat{\boldsymbol{\Omega}}_z$ is the estimated covariance matrix of the common shock component (i.e., the unobserved heterogeneity component) vector $\boldsymbol{z}_{\boldsymbol{\tau}_{t+h-k}}$, $\hat{\omega}_{jj,z}$ is the jth diagonal element of $\hat{\boldsymbol{\Omega}}_z$. In our application of liquidity risk network, and $\tilde{C}^{z}_{i\leftarrow j,h,\boldsymbol{\tau}}$ represents how much of bank i's future liquidity uncertainty (at horizon h) is due to liquidity shocks to the unobserved heterogeneity of bank j conditioning on the specific future scenario $\boldsymbol{\tau}$. Note that the diagonal element $\tilde{C}^{z}_{i\leftarrow i,h,\boldsymbol{\tau}}$ measures the self-link, how much of bank i's future liquidity uncertainty (at horizon h) is due to liquidity shocks to its own unobserved heterogeneity based on the scenario $\boldsymbol{\tau}$.

Then we row-normalize the matrix $(\tilde{C}^{z}_{i\leftarrow j,h,\boldsymbol{\tau}})$, denoted as $(C^{z}_{i\leftarrow j,h,\boldsymbol{\tau}})$ with $C^{z}_{i\leftarrow j,h,\boldsymbol{\tau}} = \frac{\tilde{C}^{z}_{i\leftarrow j,h,\boldsymbol{\tau}}}{\sum_{j=1}^{N} \tilde{C}^{z}_{i\leftarrow j,h,\boldsymbol{\tau}}}$. Next, we compute total directional connectedness including "To", "From," and "Net" measures. Specifically, "To" measure represents the total directional connectedness from bank i *to others* defined as

$$C^{z}_{\bullet\leftarrow i,h,\boldsymbol{\tau}} = \sum_{j=1,j\neq i}^{N} C^{z}_{j\leftarrow i,h,\boldsymbol{\tau}}. \tag{19}$$

Similarly, "From" measure represents the total directional connectedness *from others* to bank i, defined as

$$C^z_{i\leftarrow\bullet,h,\boldsymbol{\tau}} = \sum_{j=1,j\neq i}^{N} C^z_{i\leftarrow j,h,\boldsymbol{\tau}}. \tag{20}$$

Finally, we compute total connectedness, also known as system-wide connectedness, defined as

$$C^z_{h,\boldsymbol{\tau}} = \frac{1}{N} \sum_{i,j=1,i\neq j}^{N} C^z_{i\leftarrow j,h,\boldsymbol{\tau}}. \tag{21}$$

3.3.3 Quantile connectedness based on combined shocks

In this section, we define overall quantile connectedness based on combined shocks which is combining idiosyncratic shocks and common shocks, in a similar way as the separate quantile connectedness measures. Let $\tilde{C}_{i\leftarrow j,h,\boldsymbol{\tau}}$ denote the proportion of bank i's h-step-ahead generalized forecast error variance due to shocks to either the idiosyncratic component or the unobserved heterogeneity of bank j, conditional on the future scenario $\boldsymbol{\tau} = (\boldsymbol{\tau}_t, ..., \boldsymbol{\tau}_{t+h})$ (alternatively, $\boldsymbol{\tau}_t \to \boldsymbol{\tau}_{t+1} \to \cdots \to \boldsymbol{\tau}_{t+h}$), defined as

$$\tilde{C}_{i\leftarrow j,h,\boldsymbol{\tau}} = \frac{\sum_{k=0}^{h-1} \hat{\omega}_{jj}^{-1} \left(l_i' \hat{\Phi}_k \hat{\boldsymbol{\Omega}} l_j\right)^2}{\sum_{k=0}^{h-1} \left(l_i' \hat{\Phi}_k \hat{\boldsymbol{\Omega}} \hat{\Phi}_k' l_i\right)}, \qquad i = 1, 2, \cdots, N;\ j = 1, 2, \cdots, N, \tag{22}$$

where $\hat{\boldsymbol{\Omega}}$ equals $\hat{\boldsymbol{\Omega}}_e + \hat{\boldsymbol{\Omega}}_z$, $\hat{\omega}_{jj}$ is the jth diagonal element of $\hat{\boldsymbol{\Omega}}$. In our application of liquidity risk network, the above $\tilde{C}_{i\leftarrow j,h,\boldsymbol{\tau}}$ represents how much of bank i's future liquidity uncertainty (at horizon h) is due to liquidity shocks to either the idiosyncratic component or the unobserved heterogeneity of bank j conditioning on the specific future scenario $\boldsymbol{\tau}$. Note that the diagonal element $\tilde{C}_{i\leftarrow i,h,\boldsymbol{\tau}}$ measures the self-link, how much of bank i's future liquidity uncertainty (at horizon h) is due to liquidity shocks to its own idiosyncratic component or unobserved heterogeneity based on the scenario $\boldsymbol{\tau}$.

Then we row-normalize the matrix $(\tilde{C}_{i\leftarrow j,h,\boldsymbol{\tau}})$, denoted as $(C_{i\leftarrow j,h,\boldsymbol{\tau}})$ with $C_{i\leftarrow j,h,\boldsymbol{\tau}} = \frac{\tilde{C}_{i\leftarrow j,h,\boldsymbol{\tau}}}{\sum_{j=1}^{N} \tilde{C}_{i\leftarrow j,h,\boldsymbol{\tau}}}$. Next, we compute total directional connectedness including "To", "From," and "Net" measures. Specifically, "To" measure represents the total directional connectedness from bank i *to others* defined as

$$C_{\bullet\leftarrow i,h,\boldsymbol{\tau}} = \sum_{j=1,j\neq i}^{N} C_{j\leftarrow i,h,\boldsymbol{\tau}}. \tag{23}$$

Similarly, "From" measure represents the total directional connectedness *from others* to bank i, defined as

$$C_{i\leftarrow\bullet,h,\boldsymbol{\tau}} = \sum_{j=1,j\neq i}^{N} C_{i\leftarrow j,h,\boldsymbol{\tau}}. \tag{24}$$

Finally, we compute total connectedness, also known as system-wide connectedness, defined as

$$C_{h,\boldsymbol{\tau}} = \frac{1}{N} \sum_{i,j=1,i\neq j}^{N} C_{i\leftarrow j,h,\boldsymbol{\tau}}. \tag{25}$$

3.4 Computational implementation

This section summarizes how to obtain the measures numerically. As discussed above, we can estimate the model (1) at a given conditional quantile. In our empirical analysis, we set $\tau = \{0.01, 0.02, ..., 0.99\}$, and the model (1) is estimated at each quantile point. Let H be the number of posterior samples. This produces

$$\{B_{\tau}^{(a)}, F_{\tau}^{(a)}, \Lambda_{\tau}^{(a)}, z_{it,\tau}^{(a)}, G_{e_i}^{-1}(\tau)^{(a)} | \tau = 0.01, ..., 0.99, a = 1, ..., H\}$$

with $z_{it,\tau}^{(a)} = \boldsymbol{f}_{t,\tau}^{(a)\prime} \boldsymbol{\lambda}_{i,\tau}^{(a)}$. Here a denotes a-th generated posterior sample.

Let h be a forecast horizon and $\boldsymbol{\tau}_t = (\tau_{1,t}, ..., \tau_{N,t})'$,..., $\boldsymbol{\tau}_{t+h} = (\tau_{1,t+h}, ..., \tau_{N,t+h})'$ be the vector of quantile points specifying the future scenario. With these generated posterior samples, we can calculate various quantities in regard to the connectedness measures proposed in the previous sections. To calculate (18), we need to estimate $\boldsymbol{\Omega}_z$. Because the time index $k > t$ indicates a future time point, we construct this quantity by taking unconditional posterior expectation across sample periods by using bootstrap sampling from the posterior samples. Then, $\hat{\boldsymbol{\Omega}}_z$ can be constructed by

$$\hat{\boldsymbol{\Omega}}_z^{(a)} = \frac{1}{99T} \sum_{\tau=0.01}^{0.99} \sum_{t=1}^{T} \left(\boldsymbol{z}_{t,\tau}^{(a)} - \hat{\boldsymbol{z}}_t \right) \left(\boldsymbol{z}_{t,\tau}^{(a)} - \hat{\boldsymbol{z}}_t \right)', \tag{26}$$

where $\boldsymbol{z}_{t,\tau}^{(a)} = (z_{1,t,\tau}^{(a)}, ..., z_{N,t,\tau}^{(a)})'$ and $\hat{\boldsymbol{z}}_t = \frac{1}{99T} \sum_{\tau=0.01}^{0.99} \sum_{t=1}^{T} \boldsymbol{z}_{t,\tau}^{(a)}$ is a proxy of unconditional mean of the unobserved heterogeneity. Let $\Phi_{t+h,k}^{(a)}$ be constructed based on the a-th posterior sample. Then we have $\hat{\Phi}_k \hat{\boldsymbol{\Omega}}_z = \frac{1}{H} \sum_{a=1}^{H} \Phi_{t+h,k}^{(a)} \hat{\boldsymbol{\Omega}}_z^{(a)}$ and $\hat{\Phi}_k \hat{\boldsymbol{\Omega}}_z \hat{\Phi}_k' = \frac{1}{H} \sum_{a=1}^{H} \Phi_{t+h,k}^{(a)} \hat{\boldsymbol{\Omega}}_z^{(a)} \Phi_{t+h,k}^{(a)\prime}$. Therefore, we can compute these proposed scenario-based quantile connectedness measures based on the unobserved heterogeneity component. Similarly, we can construct $\hat{\boldsymbol{\Omega}}_e$ and compute these proposed scenario-based quantile connectedness measures based on the idiosyncratic component as defined in (14), and also the overall quantile connectedness measure based on the idiosyncratic component and unobserved heterogeneity together.

Remark 7 Unlike the previous studies Cecchetti and Li (2008) and Ando et al. (2022b), our approach does not require the quantile τ to be identical across individual units as well as throughout the forecasting time horizon. This result is useful when we construct quantile connectedness under various future scenarios.

4 Asymptotic theory

Let $\vartheta_\tau \equiv \{B_\tau, F_\tau, \Lambda_\tau\}$ denote the parameter in the model (10). Our concern here is the sequence of posterior distributions $\pi(\vartheta_\tau|Y, X)$ constructed by the size of $T \times N$ panel data as $N, T \to \infty$. In this paper, we show that the constructed posterior density is Hellinger consistent sequence. Hellinger distance is a useful tool to establish the posterior consistency (Barron et al. (1999), Ghoshal et al. (1999), Walker and Hjort (2001)). For two density functions $s(y)$ and $g(y)$, Hellinger distance is defined as

$$H(g, s) = \frac{1}{2}\left\{\int (g^{1/2}(y) - s^{1/2}(y))d(y)\right\}^2.$$

Recall our pseudo-likelihood based density function:

$$f(Y|X, \vartheta_\tau) \propto \exp\left[-\frac{1}{NT}\sum_{i=1}^{N}\sum_{t=1}^{T} q_{it,\tau}(\vartheta_\tau)\right],$$

where we used a simplified notation $q_{it,\tau}(\vartheta_\tau)$ such that $q_{it,\tau}(\vartheta_\tau) \equiv q_\tau(y_{it} - \boldsymbol{x}_t'\boldsymbol{b}_{i,\tau} - \boldsymbol{f}_{t,\tau}'\boldsymbol{\lambda}_{i,\tau})$. We establish Bayesian consistency under the pseudo-likelihood $f(Y|X, \vartheta_\tau)$, in the sense that, for any $\mu > 0$,

$$\pi_{N,T,\tau}\left(\{\vartheta_\tau : H(f(Y|X, \vartheta_\tau), f(Y|X, \vartheta_{\tau,0})) > \mu\}\right) \to 0 \quad as\ N, T \to \infty, \tag{27}$$

where $\vartheta_{\tau,0}$ is true value of ϑ_τ. Here $\pi_{N,T,\tau}(\cdot)$ is defined as

$$\pi_{N,T,\tau}(A) = \int_A \frac{f(Y|X, \vartheta_\tau)}{f(Y|X, \vartheta_{\tau,0})}\pi(\vartheta_\tau)d\vartheta_\tau,$$

where A is the subset of parameter space of ϑ_τ. To obtain the claim (27), we assume the following conditions.

Assumptions

We denote the true regression coefficient as $\boldsymbol{b}_{i,0,\tau}$. Similarly, we denote $F_{0,\tau} = (\boldsymbol{f}_{1,0,\tau}, ..., \boldsymbol{f}_{T,0,\tau})'$ and $\Lambda_{0,\tau} = (\boldsymbol{\lambda}_{1,0,\tau}, ..., \boldsymbol{\lambda}_{N,0,\tau})'$ as the true factors and loadings. A set of regularity conditions for establishing the the claim (27) are given as follows.

Assumption A: Common factors

Let $\mathcal{F}$ be a compact subset of R^{r_τ}. The common factors $\boldsymbol{f}_{t,0,\tau} \in \mathcal{F}$ satisfy $T^{-1}\sum_{t=1}^{T} \boldsymbol{f}_{t,0,\tau}\boldsymbol{f}'_{t,0,\tau} = I_{r_\tau}$.

Assumption B: Factor loadings and regression coefficients

(B1) Let $\mathcal{B}$ and $\mathcal{L}$ be compact subsets of $\mathbb{R}^{Np+1}$ and $\mathbb{R}^{r_\tau}$, respectively. The regression coefficient $\boldsymbol{b}_{i,0,\tau}$ and the factor-loading $\boldsymbol{\lambda}_{i,0,\tau}$ satisfy that $\boldsymbol{b}_{i,0,\tau} \in \mathcal{B}$ and $\boldsymbol{\lambda}_{i,0,\tau} \in \mathcal{L}$ for each i.

(B2) The factor-loading matrix $\Lambda_{0,\tau} = (\boldsymbol{\lambda}_{1,0,\tau}, \ldots, \boldsymbol{\lambda}_{N,0,\tau})'$ satisfies $N^{-1}\sum_{i=1}^{N} \boldsymbol{\lambda}_{i,0,\tau}\boldsymbol{\lambda}'_{i,0,\tau} \xrightarrow{p} \Sigma_{\Lambda_\tau}$, where Σ_{Λ_τ} is an $r_\tau \times r_\tau$ positive definite diagonal matrix with diagonal elements distinct and arranged in the descending order.

Assumption C: Idiosyncratic error terms

(C1): The random variable

$$\varepsilon_{it,\tau} = y_{it} - \sum_{h=1}^{p}\sum_{j=1}^{N} b_{ijh,0,\tau} y_{j,t-h} - \sum_{k=1}^{r} f_{tk,0,\tau}\lambda_{ik,0,\tau} - G^{-1}_{e_{it}}(\tau)$$

satisfies $P(\varepsilon_{it,\tau} \leq 0) = \tau$, and is independently distributed over i and t, conditional on X_t, $B_{0,\tau}$, $F_{0,\tau}$ and $\Lambda_{0,\tau}$.

(C2): The conditional density function of $\varepsilon_{it,\tau}$ given $(X_t, B_{0,\tau}, F_{0,\tau}, \Lambda_{0,\tau})$, denoted as $g_{it}(\varepsilon_{it,\tau})$, is continuous. In addition, for any compact set $\mathcal{C}$, there exists a positive constant $\underline{g} > 0$ (depending on $\mathcal{C}$) such that $\inf_{c\in\mathcal{C}} g_{it}(c) \geq \underline{g}$ for all i and t.

Assumption D: Explanatory variables and design matrix

(D1): For a positive constant C_x, explanatory variables satisfy $\sup_{it} \|\boldsymbol{x}_{it}\| \leq C_x$ almost surely.

(D2): Let $\boldsymbol{X}_{i,\tau} = (\boldsymbol{x}_{i1}, \boldsymbol{x}_{i2}, \ldots, \boldsymbol{x}_{iT})'$. Define $A_{i,\tau} = \frac{1}{T}\boldsymbol{X}'_{i,\tau}M_{F_\tau}\boldsymbol{X}_{i,\tau}$, $B_{i,\tau} = (\boldsymbol{\lambda}_{i,0,\tau}\boldsymbol{\lambda}'_{i,0,\tau}) \otimes I_T$, $C_i = \frac{1}{\sqrt{T}}[\boldsymbol{\lambda}_{i,0,\tau} \otimes (M_{F_\tau}\boldsymbol{X}_{i,\tau})]'$, $\boldsymbol{\eta} = \frac{1}{\sqrt{T}}\text{vec}(M_{F_\tau}F_{0,\tau})$, and $M_{F_\tau} = I - F_\tau(F'_\tau F_\tau)^{-1}F'_\tau$. Let $\mathscr{F}_\tau$ be the collection of F_τ such that $\mathscr{F}_\tau = \{F_\tau : F'_\tau F_\tau/T = I_{r_\tau}\}$. We assume that with probability approaching one,

$$\inf_{F_\tau\in\mathscr{F}_\tau} \lambda_{\min}\left[\frac{1}{N}\sum_{i=1}^{N} E_{i,\tau}(F_\tau)\right] > 0,$$

where $\lambda_{\min}(A)$ denotes the smallest eigenvalue of matrix A, and $E_{i,\tau}(F_\tau) = B_{i,\tau} - C'_{i,\tau}A^{-1}_{i,\tau}C_{i,\tau}$.

(D3): Let $\mathcal{V}_\tau(B_\tau)$ be the $N \times T$ matrix with its (i,t)th entry equal to $\boldsymbol{x}_{it}'\boldsymbol{b}_{i,\tau}$, where $B_\tau = (\boldsymbol{b}_{1,\tau}, \boldsymbol{b}_{2,\tau}, \ldots, \boldsymbol{b}_{N,\tau})'$. There exists $c > 0$ such that

$$\frac{1}{NT}\|M_{\Lambda_{0,\tau}}\mathcal{V}_\tau(B_\tau)M_{F_{0,\tau}}\|^2 \geq c\frac{1}{N}\sum_{i=1}^{N}\|\boldsymbol{b}_{i,\tau}\|^2,$$

where $M_{\Lambda_{0,\tau}} = I - \Lambda_{0,\tau}(\Lambda_{0,\tau}'\Lambda_{0,\tau})^{-1}\Lambda_{0,\tau}'$.

(D4): For each i, there exists $c > 0$ such that with probability approaching one,

$$\liminf_{T\to\infty} \lambda_{\min}\Big(\frac{1}{T}\boldsymbol{X}_{i,\tau}'M_{F_{0,\tau}}\boldsymbol{X}_{i,\tau}\Big) \geq c.$$

Assumption E: Stationarity

(E1) Define $U_k \equiv \{\boldsymbol{u}_t, \boldsymbol{u}_{t-1}, ..., \boldsymbol{u}_{t-k}\}$ and $N \times N$ matrix $\Phi_{t,k}(U_k) \equiv \Phi_{t,k}(\boldsymbol{u}_t, \boldsymbol{u}_{t-1}, ..., \boldsymbol{u}_{t-k})$. Then,

$$\left[\sum_{k=0}^{\infty}\text{abs}\left[\Phi_{t,k}(U_{t-k})\right]\right]$$

is uniformly bounded in row sums and column sums. Here, $\text{abs}[A]_{ij} = |a_{ij}|$ for a matrix A with its (i,j)th element being a_{ij}.

(E2) The idiosyncratic error $e_{it,u_{it}}$ in (10) is stationary time series for each i.

Assumption F: Kullback–Leibler property

Let $K_v(\vartheta_{\tau,0})$ be a Kullback–Leibler neighborhood of $\vartheta_{\tau,0}$ such that, for each given $v > 0$, ϑ_τ satisfies

$$\int \log\{f(Y|X,\vartheta_{\tau,0})/f(Y|X,\vartheta_\tau)\}f(Y|X,\vartheta_{\tau,0})dY < v.$$

Then, the prior density $\pi(\vartheta_\tau)$ puts positive mass on all Kullback–Leibler neighborhood of the pseudo-likelihood based density under the true value $f(Y|X,\vartheta_{\tau,0})$:

$$\pi(K_v(\vartheta_{\tau,0})) > 0.$$

Remark 8 Assumptions A and B are consistent with our normalization conditions in (9). Assumption (C1) may be relaxed to allow the serial dependency, but we do not pursue this direction in this paper. Assumptions (C2) is standard in the quantile models. Assumption D is imposed for the identification of parameters. Assumption (D2) is imposed for the identification of $\Lambda_\tau F_\tau'$. This assumption was used in several previous studies, such as Ando et al. (2022a, 2023). Assumption (D3) can be interpreted as an extended version of Assumption A of Bai (2009). Together with Assumptions (D2) and (D3), Assumption (D4) provides the identification conditions in the

interactive-effects models Ando et al. (2023). Assumption (E1) is similar to Assumption 6 of Yu et al. (2008). It may be possible to relax Assumption (E1) and (E2) by employing an idea from the frequentist framework (e.g., Miao et al. (2020)). However, it is not our main focus here. Assumption F is necessary to encompass the true model in our model space.

The following theorem ensures that the constructed posterior based on the pseudo-likelihood based density function $f(Y|X,\vartheta_\tau)$ is Hellinger consistent sequence.

Theorem 2 *Under Assumptions A–F and $N/T \to 0$, then (27) holds.*

Remark 9 Technical proof of Theorem 2 is given in the appendix. Although our proof relies on a technique originally considered by Schwartz (1965), we note that Theorem 2 is proved under the diverging number of parameters in the sense that the dimension of parameters increases as $N,T \to \infty$. Together with the non-smoothness of the pseudo-likelihood based density function $f(Y|X,\vartheta_\tau)$ in terms of ϑ_τ, it is not straightforward task to establish Theorem 2. To overcome the non-smoothness, we first had to establish the following together with the restriction $N/T \to 0$ and the empirical process theory (van der Vaart and Wellner (1996), see also Ando and Bai (2020)):

$$\sup_{\forall t,\boldsymbol{f}_t\in\mathcal{F},\forall i,\boldsymbol{\lambda}_i\in\mathcal{L},\boldsymbol{b}_i\in\mathcal{B}} \left| \frac{1}{NT}\sum_{i=1}^{N}\sum_{t=1}^{T} q_\tau\Big(y_{it}-\boldsymbol{x}_{it}'\boldsymbol{b}_{i,\tau}-\boldsymbol{f}_{t,\tau}'\boldsymbol{\lambda}_{i,\tau}\Big) - E\Big[q_\tau\Big(y_{it}-\boldsymbol{x}_{it}'\boldsymbol{b}_{i,\tau}-\boldsymbol{f}_{t,\tau}'\boldsymbol{\lambda}_{i,\tau}\Big)\Big] \right| = o_p(1),$$

where $E(\cdot)$ is the expectation of y_{it} conditioned on X, $F_{0,\tau}$, $\Lambda_{\tau,0}$ and $B_{\tau,0}$. The restriction $N/T \to 0$ is also imposed by Ghosh et al. (2019) to establish the posterior consistency for the high-dimensional "mean" vector autoregressive (VAR) model with Gaussian idiosyncratic errors. Ghosh et al. (2019) also allowed the dimension of individual units grows with the length of time series. Thus, our assumption $N = o(T)$ is not restrictive because this condition is also necessary for the high-dimensional "mean" VAR case.

5 Empirical Analysis

In this empirical analysis section, we evaluate the interbank liquidity risk network by implementing both the baseline fixed-quantile connectedness approach and the scenario-based quantile connectedness approach. We assume that the data is generated from the structure in (10). In the fixed-quantile analysis, we study the network connectedness for various quantiles, mainly focusing on two sample periods (before and during the COVID-19 pandemic). In the scenario-based quantile analysis, we pre-specify the scenario based on the Repo crisis during September

2019. We also investigate the connectedness measures based on different types of shocks (idiosyncratic shocks, common shocks, and combined shocks). Further, we look into the dynamic evolution of the quantile liquidity risk network by using a rolling window estimation.

5.1 Fixed-quantile connectedness

In the baseline results, we study the liquidity risk network of twelve large U.S. banks over the period 2017 to 2020, with the list of banks provided in Table 1 and data details described in Section 2. We focus on special scenarios, where the quantile point is fixed (the same) across individual banks and throughout the forecast horizon, by considering five different percentiles: 5th, 25th, 50th, 75th and 95th. We first estimate the model using the proposed Bayesian nuclear norm approach. Then based on the Bayesian estimates, the quantile network connectedness measures are computed by generalizing the forecast error variance decomposition method in Diebold and Yilmaz (2014) from the conditional mean to quantiles. The details of methodology are described in Section 3.3. The liquidity network connectedness measures include total connectedness, pairwise directional connectedness, bank-specific systemic importance, and vulnerability, which are useful for bank supervision and financial stability monitoring.

We consider both the static and dynamic estimation of the liquidity risk network. In the static approach, we estimate the liquidity network connectedness based on two sub-samples (before and during the COVID-19 pandemic). The estimated network is also compared across quantiles. In the dynamic approach, we estimate the time-varying liquidity network by rolling window estimation. Dynamic network estimation allows us to examine the continuous real-time evolution of the liquidity network. Due to space constraints, the dynamic network results are provided in the appendix.

We first apply the proposed Bayesian nuclear norm approach to estimate the model (1) with lag $p = 1$ determined by both AIC and BIC. Then using the QVAR estimates, we compute quantile connectedness measures at horizon $H = 12$ following the methodology in Section 3.3.[9] Our analysis considers three types of quantile connectedness as defined in Section 3.3: network based on idiosyncratic shocks, network based on common shocks (through unobserved heterogeneity), and overall network based on combined shocks (combining idiosyncratic shocks and common shocks). Our analysis focuses on three main quantile connectedness measures: total connectedness, pairwise directional connectedness, and total directional connectedness including To, From, and Net.

[9]Horizon $H = 12$ is commonly used in the literature of measuring network connectedness based on variance decomposition. For robustness check, we have also examined a range of nearby horizon values, which produce similar results. This finding is consistent with Diebold and Yilmaz (2014).

5.1.1 Connectedness based on idiosyncratic shocks

Total Connectedness

Table 2 reports the total connectedness across quantiles, before and during the COVID-19 pandemic. Total connectedness measures the average strength of liquidity shocks transmission across banks. There are two main findings from the results. Relative to the pre-COVID period, the magnitude of total connectedness is higher during the pandemic (almost 50% larger), consistent across quantiles, indicating that a liquidity shock to one bank would have a larger impact on other banks during the pandemic. This might be due to the stressed market condition during pandemic, where the liquidity funding market was overall more constrained, so an idiosyncratic liquidity shock hitting one bank generated more spillover to affect another banks liquidity uncertainty.

Another finding is that total connectedness is higher at the tails, both the lower 5th and upper 95th tails where the idiosyncratic shocks are relatively larger compared to these at the median. This implies that a bank hit by a large idiosyncratic liquidity shock (or a tail shock) could transmit a higher degree of spillover effect to another banks liquidity uncertainty, compared to an average size shock (at the center of the distribution). Larger shocks happening at tails are often defined in relation to shocks that propagate during rare events relative to normal times. In our example tail shocks generate larger spillover effects or shocks propagation in the system.

Pairwise Directional Connectedness

Pairwise Directional Connectedness measures how liquidity shocks are transmitted across banks. The (i, j) entry in each connectedness table represents how much of bank i's future LCR uncertainty is due to idiosyncratic shocks coming from bank j's LCR today as the shock size varies (across quantiles). This indicates how idiosyncratic shocks of different sizes transmit from a bank to affect anther banks LCR uncertainty in the future.

Due to the confidentiality of the data, we aggregate the bank-level pairwise directional connectedness into group-level pairwise directional connectedness, where the twelve banks are classified into three groups: Big4 banks (BAC, C, JPM, WFC), other domestic banks (BK, GS, MS, STT), and foreign banks (BARC, CS, DB, UBS). The aggregated results are provided in Table 3. The aggregation is based on the following formula

$$C^{H}_{G_m \leftarrow G_n, \tau} = \frac{1}{4} \sum_{i \in G_m, j \in G_n} C^{H}_{i \leftarrow j, \tau}, \tag{28}$$

where G_m denotes the mth group, "Big4 banks", "Other domestic banks," or "Foreign banks"; similar for G_n; and $C^{H}_{i \leftarrow j, \tau}$ is the bank-level pairwise directional connectedness from bank j to

bank i. The above $C^{H}_{G_m \leftarrow G_n, \tau}$ measures the fraction of (group m) banks' future LCR uncertainty that is due to shocks to (group n) banks' LCR.

The group-level pairwise directional connectedness measures provide useful insights into the liquidity risk network structure: how do idiosyncratic liquidity shocks of different sizes in one bank group relate to upcoming liquidity uncertainty in another bank group? The results are reported in Table 3, where each entry (m, n) in the table measures the strength of shocks transmission from group n in the column to group m in the row. In other words, the column group represents the shocks exporter while the row group represents shocks receiver. The heterogeneity across groups increases during the pandemic. Before the pandemic, self-links (the diagonal elements) are dominating cross-bank links (the off-diagonal elements). In other words, near-term (12 trading days in the future) liquidity uncertainty before the pandemic is most associated with idiosyncratic changes that hit the same bank group in the current period. The dominance becomes weaker at the tails than at the median, implying when the liquidity profile of the bank system deviates from normal (or larger idiosyncratic shocks under rare events), spillover effects across banks become larger due to their increased connections.

However, during the pandemic, cross-bank links are much more substantial than self-links, indicating that those same idiosyncratic changes were more related to liquidity uncertainty in other bank groups. The idiosyncratic liquidity shock transmits across the network more, in other words, spillover effect plays a more important role in liquidity risk transmission during the pandemic. In addition, cross-links are more substantial at the tails (associated with larger shocks or rare events), indicating that larger idiosyncratic shocks generate more shocks propagation across the network during the pandemic when the market was under stress.

Second, we find some clustering during the pandemic. At the tails during the pandemic, shock exporters (column groups) are clustered at a few banks (Big4 and Other domestic banks) where shocks to their liquidity are affecting almost all other banks in the system. In particular, Big4 banks export shocks at the upper 95th tail: liquidity shocks at the Big4 banks are most associated with near-term liquidity uncertainty in all the bank groups. In contrast, Other domestic banks are the main shock exporters at the lower 5th tail. Foreign banks do not play a significant role in exporting shocks except at the median (normal times). Compared to the tails, the shocks exporters are slightly less clustered at the 25th and 75 percentiles.

Differences in how these bank groups export liquidity shocks are likely due to large differences in their relative sizes and business models. At shown in Table 1, the average size of Big4 is much larger than Other domestic banks and Foreign banks, while Other domestic banks and Foreign banks hold much less loans as share of assets and generate much more of their earnings

from activities outside of traditional banking (noninterest income/assets). Compared to Other domestic banks, Foreign banks generate even more noninterest income as share of assets than Other domestic banks (average is 5.5% versus 3.6%). In addition, Foreign banks in our sample are subsidiaries of international GSIBs, which likely affects their propensity to receive or transmit shocks. There is no clear clustering pattern for shocks importers.

Total Directional Connectedness

Based on the pairwise directional connectedness, we compute the total directional connectedness including To, From, and Net measures. Specifically, the To measure of bank i represents the total amount of future liquidity uncertainty of other banks that is associated with liquidity shocks at bank i. It measures a bank's tendency to *export* shocks *to* other banks. The From measure of bank i represents the amount of bank i's future liquidity uncertainty that is associated with liquidity shocks from other banks: how much a bank *imports* shocks *from* other banks. The Net measure is the difference between the To and From measures, computed as To measure minus From measure. A positive Net measure means that the bank is a net shocks exporter (the shocks it exports to others is more than the shocks it imports from others). Similarly, a negative Net measure means that the bank is a net shocks importer (importing more shocks than exporting shocks). Economically, the To and From measures represent bank-specific systemic importance (in terms of exporting shocks *to* other banks) and vulnerability (in terms of importing shocks *from* other banks), respectively, which could provide useful insights for supervisors. Similar to the results in Table 3, we also aggregate bank-level total directional connectedness into group-level total directional connectedness measures, provided in Table 4.

Several relationships are revealed in Table 4. First, looking at the results of the To measure, consistent with the findings from the pairwise directional connectedness results in Table 3, at the tails during the pandemic, domestic banks (Big4 and Other domestic banks) tend to export more liquidity uncertainty shocks compared to Foreign banks, indicating domestic banks have larger systemic impacts. Before the pandemic, the relationships were more consistent across the distribution. But the leading liquidity shocks exporters are not the same across quantiles. For example, during the pandemic, Big4 banks are the leading risk exporters at the upper 95th tail, while Other domestic banks are the leading risk exporters at the lower 5th tail. This might be due to the large differences in their relative sizes and business models as discussed in the previous section of pairwise connectedness results and in Table 1.

Second, relative to the To measure, there is less heterogeneity for the From measure across quantiles and between pre-COVID and COVID periods. Before the pandemic, Foreign banks

have smaller From measures compared to domestic banks, meaning Foreign banks are less vulnerable to liquidity shocks from other banks. During the pandemic, Foreign banks become more vulnerable, especially at the tails, with a similar magnitude as domestic banks. Overall, the level of bank vulnerability to other banks' liquidity shocks is higher during the pandemic than pre-pandemic. In other words, the spillover effect of liquidity shocks is greater during the pandemic.

The Net measure is summarized in the bottom panel of Table 4, where green denotes negative values meaning the bank is a net shocks importer, while red denotes positive values meaning the bank is a net shocks exporter. The results are quite different before and during the pandemic, as well as across bank groups. Comparing domestic and Foreign banks, on average, domestic banks are net shocks importers before the pandemic but then become net shocks exporters during the pandemic. The results suggest that before the pandemic, Big4 banks served as a liquidity buffer for the banking system, absorbing shocks and helping the system. During the pandemic, Big4 banks still absorbed shocks as their "From" measure is still high, but their "To" measure increased more, making them net shocks exporters.

It is the opposite for Foreign banks. Though Foreign banks are net shocks exporters before pandemic, their Net measure is low, and it is positive mainly because of their low From measure. The reason for low From measure might be that, they are subsidiaries of international GSIBs and relatively smaller compared to the domestic banks in our sample. When the pandemic came, the overall interconnectedness among banks has increased, so Foreign banks receive more liquidity uncertainty shocks as shown in their From measure that the measure has increased substantially during the pandemic which drives their Net measure to be negative.

Comparing Big4 and Other domestic banks during pandemic, on average, Big4 banks are net shocks exporters at the 95th percentile, while Other domestic banks are net shocks exporters at the 5th percentile. Differences in how these two bank groups share liquidity shocks are likely due to large differences in their relative sizes and business models as discussed in the previous section of pairwise connectedness results and shown in Table 1.

In addition, the substantial change of the Net measure before and after the pandemic is similar to that of the To measure. The main reason is the magnitude of the From measure is relatively small compared to the To measure. Therefore, the majority of the Net measure comes from the To measure, and thus they have a similar pattern.

5.2 Dynamic estimation of the network connectedness

In this section, we provide results of the time-varying liquidity network using a rolling window estimation with a 250-day window, related to the baseline analysis where the quantile point is fixed across banks and throughout the forecast horizon.[10] In this section, due to space, we only present the time-varying results based on idiosyncratic shocks. The results based on common shocks and combined shocks show similar findings.

Figure 1 presents the dynamics of total connectedness across quantiles, where both mean and standard deviation (SD) are reported for each quantile. Overall the strength of total connectedness is higher at the tails than at the median, implying that when the bank system deviates from normal, total connectedness increases. This is consistent with the finding in the static approach. However, interestingly we find the SD of total connectedness is larger at the median than at the tails, indicating that when the system is normal, total connectedness is more volatile compared to that when the system is far away from normal. In addition, the time-varying total connectedness at the median shows two cycles: one starting in early 2018 and ending in mid-2019, whereas the second coincides with the COVID-19 pandemic from about April/May 2020 and trending up towards the end of 2020. In contrast, when the system deviates from normal, the system is overall more interconnected and does not show significant cycles.

We also compute total directional connectedness for each bank, and then aggregate it to group level. The time series plots of To and From measures by bank group are provided in Figures 3-5 in the appendix. Regarding the To measure, Other domestic banks have the most volatile To measure while Foreign banks have the least. Consistently across bank groups, the To measure is much more volatile at the tails than at the median. In contrast, the From measure is less volatile than the To measure. However, Other domestic banks still have the most volatile From measure compared to the other two groups.

5.3 Scenario-based quantile connectedness

Different from the fixed-quantile network connectedness analysis, we measure scenario-based quantile connectedness in this section by pre-specifying the future economic scenario which is used in the forecast error variance decomposition. We specify the future economic scenario being the Repo crisis in September 2019, and then estimate the model using the liquidity data before the Repo crisis. Based on the model estimates, we compute network connectedness measures following the methodology proposed in Section 3.3 by focusing on the three main measures:

[10] As shown in Diebold and Yilmaz (2014), they have considered a range of windows sizes and find they produce similar results. For robustness check, we have also examined a range of nearby window sizes, which produce similar results as well.

total (or system-wide) connectedness, pairwise directional connectedness, and total directional connectedness (To, From, and Net).

More specifically, we first estimate the QVAR model using the proposed Bayesian nuclear norm estimation approach (described in Section 3) based on the data before the Repo crisis and then compute the scenario-based quantile connectedness measures based on the Bayesian estimates (following the methodology presented in Section 3.3). In terms of specifying the scenario, let t be the U.S. repo market shock day that happened on September 17, 2019. Based on the actual LCR data, we compute the percentiles of individual bank's LCR level on that day t, as well as the following H days $(t+1, t+2, \ldots, t+H)$ ($H = 12$ in our analysis), relative to that bank's own historical distribution. This gives us a scenario-specific quantile path (i.e., according to the notation $(\boldsymbol{\tau}_t, \boldsymbol{\tau}_{t+1}, \ldots, \boldsymbol{\tau}_{t+12})$ used in Section 3.3). Finally, we estimate network connectedness measures based on this particular scenario, using the formulas developed in Section 3.3.

Table 5 presents the three main connectedness measures at group level, according to different types of shocks. From left to right, the network connectedness is based on idiosyncratic shocks, common shocks, and combined shocks (combining idiosyncratic shocks and common shocks). From top to bottom, we first report total/system-wide connectedness, then total directional connectedness measures (To, From, and Net), and finally pairwise directional connectedness measures. From the results, we can see that the system-wide connectedness is similar and consistently high across estimated networks based on different types of shocks, indicating that these banks are overall closely interconnected with each other during the Repo crisis.

Moving to the detailed pairwise directional connectedness measure as shown in the middle panel of Table 5, we can see there is little heterogeneity across different types of shocks, except for Other domestic banks which tend to have lower pairwise directional connectedness from themselves to other banks in the case of common shocks compared to the other two types of shocks. Overall, the liquidity risk spillovers from Big4 banks to other banks tend to be larger than the other two bank groups. In addition, we do not see the dominance of self-links (the diagonal elements), implying that cross-bank links (the off-diagonal elements) or spillovers across banks are at least as important as self-links in the liquidity risk transmission.

Turning to total directional connectedness measures, we find that different groups show different patterns. As for Big4 banks, their To measure is consistently the largest across networks based on different types of shocks, implying they are the most systemically important banks in terms of exporting liquidity shocks to other banks for both idiosyncratic shocks and common shocks. Both Other domestic banks and Foreign banks tend to have much lower To measures,

meaning they are relatively much weaker in terms of transmitting liquidity shocks to other banks. Comparing the To measure across different types of shocks, we can see that Other domestic banks are the most volatile group as they have much lower To measures in the case of common shocks compared to other two cases, while both Big4 and Foreign banks show similar magnitude of To measures across the three types of shocks. The magnitude of the From measure is close across bank groups, indicating banks' vulnerability is similar in terms of receiving shocks from other banks. Comparing To and From measures, we notice there is much less heterogeneity for the From measure across bank groups. This indicates that different banks tend to be more different in terms of their systemic importance (i.e., their ability of transmitting liquidity shocks to other banks) while they tend to be similar in terms of their vulnerability (i.e., receiving liquidity shocks from other banks). For the Net measure, we find that Big4 banks are consistently net shocks exporters (positive and red) across different types of shocks, while both Other domestic and Foreign banks tend to be net shocks importers (negative and green). Other domestic banks tend to import shocks through common shocks, whereas Foreign banks tend to import shocks through idiosyncratic shocks.

6 Conclusion

In this paper, we study the U.S. interbank liquidity risk network based on a supervisory dataset, using a scenario-based quantile network connectedness approach where the network connectedness is computed under a pre-specified future economic scenario. Specifically, we consider a QVAR model with unobserved heterogeneity, where a latent common factor structure is used to deal with unobserved heterogeneity so that the latent factor structure absorbs the part of the errors that are correlated with the regressors. We then propose a new Bayesian nuclear norm estimation method using MCMC based on Gibbs sampling. To develop the scenario-based quantile network connectedness framework, we derive a scenario-based moving average expression of QVAR, obtain the forecast error variance under the pre-specified economic scenario, and then generalize the existing forecast error variance decomposition. Moreover, the connectedness measures are defined depending on the type of shocks considered: idiosyncratic shocks (for idiosyncratic contagion network), common shocks (for common shocks induced contagion network), or combined shocks (overall shocks combining idiosyncratic and common shocks).

The proposed methodology is applied to analyze the U.S. interbank liquidity risk network focusing on the twelve large U.S. bank holding companies, using the daily supervisory FR 2052a data. We first characterize the fixed-quantile network connectedness (a special case of the proposed scenario-based quantile network framework), focusing on the comparison between pre-

and during- pandemic periods. The main finding is that the liquidity risk network varies both across quantiles and across different types of shocks considered, and has changed substantially during the COVID-19 pandemic period relative to the pre-pandemic period. Then we study the scenario-based liquidity risk network connectedness based on a particular scenario specified as the Repo crisis which happened during September 2019, and the main finding is that overall, Big4 banks play a more important role in liquidity risk transmission than other banks. The estimated quantile liquidity risk network connectedness measures could be useful for bank supervision and financial stability monitoring by providing leading indicators of the system-wide liquidity risk connectedness not only at the median but also at the tails or under a pre-specified scenario. The measures also help identify systemically important banks and vulnerable banks in the liquidity risk transmission of the U.S. banking system.

Finally, this paper generalized the forecast error variance decomposition (Diebold and Yilmaz (2014)) by using a scenario-based quantile network connectedness approach. Billio et al. (2012) developed a connectedness measure based on principal components analysis and Granger-causality tests. It is interesting to extend their study to measure the quantile connectedness by using our Bayesian QVAR framework. By using our Bayesian QVAR approach, we can also explore quantile impulse response analysis (Lee et al. (2021)). We would like to explore these topics in a future study.

References

Alter, A. and Beyer, A. (2014). "The Dynamics of Spillover Effects during the European Sovereign Debt Turmoil," *Journal of Banking and Finance*, **42**, 134–153.

Ando, T. and Bai, J. (2015). "Asset Pricing with a General Multifactor Structure," *Journal of Financial Econometrics*, **13-3**, 556–604.

Ando, T. and Bai, J. (2020). "Quantile co-movement in financial markets: A panel quantile model with unobserved heterogeneity," *Journal of the American Statistical Association*, **115**, 266–279.

Ando, T., Bai, J. and Li, K. (2022a). "Bayesian and maximum likelihood analysis of large-scale panel choice models with unobserved heterogeneity," *Journal of Econometrics*, **230**(1), 20–38.

Ando, T. Greenwood-Nimmo, M. and Shin, Y. (2022b). "Quantile Connectedness: Modelling Tail Behaviour in the Topology of Financial Networks," *Management Science*, **68**(4), 2401–2431.

Ando, T., Li, K. and Lu, L. (2023). "A spatial panel quantile model with unobserved heterogeneity," *Journal of Econometrics*, **232**(1), 191–213.

Armagan, A., Dunson, D.B., Lee, J., Bajwa, W.U. and Strawn, N. (2013). "Posterior consistency in linear models under shrinkage priors," *Biometrika*, **100**, 1011–1018.

Bai, J. (2009). "Panel data models with interactive fixed effects," *Econometrica*, **77**, 1229–1279.

Bai, J. and Ng, S.(2013). "Principal components estimation and identification of static factors," *Journal of Econometrics*, **176**, 18–29.

Bai, J. and Ng, S. (2019). "Rank regularized estimation of approximate factor models," *Journal of Econometrics*, **212**, 78–96.

Barron, A., Schervish, M. J. and Wasserman, L. (1999). "The consistency of posterior distributions in nonparametric problems," *Annals of Statistics*, **27**, 536–561.

Basu, S. and Michailidis, G. (2015). "Regularized estimation in sparse high-dimensional time series models," *Annals of Statistics*, **243**, 1535–1567.

Billio, M., Getmansky, M., Lo, A. and Pelizzon, L. (2012). "Econometric Measures of Connectedness and Systemic Risk in the Finance and Insurance Sectors," *Journal of Financial Economics*, **104**, 535–559.

Belloni, A., Chen, M., Madrid Padilla, O.H. and Wang, Z. (2023). "High dimensional latent panel quantile regression with an application to asset pricing," *Annals of Statistics*, forthcoming.

Bontemps, D. (2010). "Bernstein-von mises theorems for gaussian regression with increasing number of regressors," *Annals of Statistics*, **39**, 2557–2584.

Cecchetti, S.G. and Li, H. "Measuring the Impact of Asset Price Booms Using Quantile Vector Autoregressions," Mimeo: Brandeis University February 2008.

Chernozhukov, V., Hansen, C., Liao, Y. and Zhu, Y. (2018). "Inference For Heterogeneous Effects Using Low-Rank Estimations," arXiv:1812.08089.

Diebold, F.X., and Yilmaz, K. (2014). "On the Network Topology of Variance Decompositions: Measuring the Connectedness of Financial Firms," *Journal of Econometrics*, **182**, 119–134.

Diebold, F.X., and Yilmaz, K. (2015). "Financial and macroeconomic connectedness: a network approach to measurement and monitoring," Oxford University Press.

Demirer, M., Diebold, F.X., Liu, L. and Yilmaz, K. (2018). "Estimating Global Bank Network Connectedness," *Journal of Applied Econometrics*, **33**, 1–15.

Ding, X., He, L. and Carin, L. (2011). "Bayesian Robust Principal Component Analysis," *IEEE Transactions on Image Processing*, **20**, 3419–3430.

Fan, J., Gong, W., and Zhu, Z. (2019). "Generalized high-dimensional trace regression via nuclear norm regularization," *Journal of Econometrics*, **212**, 177–202.

Feng, J. (2023). "Regularized quantile regression with interactive fixed effects," *Econometric Theory*, forthcoming.

Ghoshal, S. (1999). "Asymptotic normality of posterior distributions in high-dimensional linear models," *Bernoulli*, **5**, 315–331.

Ghoshal, S., Ghosh, J. K. and Ramamoorthi, R. V. (1999). "Posterior consistency of Dirichlet mixtures in density estimation," *Annals of Statistics*, **27**, 143–158.

Ghosh, S, Khare, K. and Michailidis, G. (2019). "High-dimensional posterior consistency in Bayesian vector autoregressive models," *Journal of the American Statistical Association*, **114**, 735–748.

Hale, G. and Lopez, J. A. (2019). "Monitoring banking system connectedness with big data," *Journal of Econometrics*, **212**, 203–220.

Hastie, T., Mazumder, R., Lee, J. and Zadeh, R. (2015). "Matrix completion and low rank svd via fast alternating least squares," *Journal of Machine Learning Research*, **16**, 3367-3402.

Ihrig, J.E., Kim, E., Vojtech, C.M., and Weinbach, G.C. (2019). "How Have Banks Been Managing the Composition of High-Quality Liquid Assets?" *Federal Reserve Bank of St. Louis Review*, **101**, 177-201.

Infante, S., Press, C., and Strauss, J. (2018). "The Ins and Outs of Collateral Re-use?" FEDS Notes 2018-12-21, Board of Governors of the Federal Reserve System (U.S.).

Infante, S., Press, C., and Saravay, Z. (2020). "Understanding Collateral Re-use in the US Financial System?" *AEA Papers and Proceedings*, **110**, 482-486.

Infante, S. and Saravay, Z. (2020). "What drives US treasury re-use?" Finance and Economics Discussion Series 2020-103. Washington: Board of Governors of the Federal Reserve System, https://doi.org/10.17016/FEDS.2020.103.

Kock, A.B. and Callot, L. (2015). "Oracle inequalities for high dimensional vector autoregressions," *Journal of Econometrics*, **186**, 325–344.

Koenker, R. and Bassett, G. (1978). "Regression Quantiles," *Econometrica*, **46**, 33–50.

Koenker, R. and Xiao, Z. (2006). "Quantile Autoregression," *Journal of the American Statistical Association*, **101**, 980–990.

Koop, G., Pesaran, H.M. and Potter, S.M. (1996) "Impulse response analysis in nonlinear multivariate models," *Journal of Econometrics*, **74**, 119–147.

Koltchinskii, V., Lounici, K., and Tsybakov, A. B. (2011). "Nuclear-norm penalization and optimal rates for noisy low-rank matrix completion," *The Annals of Statistics*, **139**, 2302-2329.

Lee, D.J., Kim, T.-H. and Mizen, P. (2021). "Impulse response analysis in conditional quantile models with an application to monetary policy," *Journal of Economic Dynamics and Control* , **127**, 104102.

Miao, K. Phillips, P.C.B and Su, L. (2020). "High-Dimensional VARs with Common Factors," *Journal of Econometrics*, **233**(1), 155–183.

Moon, H.R. and Weidner, M. (2019). "Nuclear norm regularized estimation of panel regression models," arXiv:1810.10987.

Negahban, S. and Wainwright, M. J. (2011). "Estimation of (near) low-rank matrices with noise and high-dimensional scaling," *The Annals of Statistics*, **39**, 1069-1097.

Negahban, S. N., Ravikumar, P., Wainwright, M. J., and Yu, B. (2012). "A unified framework for high dimensional analysis of m-estimators with decomposable regularizers," *Statistical Science*, **27**, 538–557.

Polson, N.G., James, G.S., and Windle, J. (2013). "Bayesian Inference for Logistic Models Using PlyaGamma Latent Variables," *Journal of the American Statistical Association*, **108**, 1339–1349.

Phillips, P.C.B. (1998). "Impulse response and forecast error variance asymptotics in nonstationary VARs," *Jounml of Econometrics*, **83**, 21–56.

Rezende, M., Styczynski, M.F., and Vojtech, C.M. (2021). "The Effects of Liquidity Regulation on Bank Demand in Monetary Policy Operations," *Journal of Financial Intermediation*, 46, 100860.

Rohde, A. and Tsybakov, A. B. (2011). "Estimation of high-dimensional low-rank matrices," *The Annals of Statistics*, **39**, 887-930.

Schüler, Y. S. (2014) "Asymmetric Effects of Uncertainty over the Business Cycle: A Quantile Structural Vector Autoregressive Approach," Working Paper 2014-02, University of Konstanz January 2014.

Schwartz, L. (1965). "On Bayes procedures," *Zeitschrift für wahrscheinlichkeitstheorie und verwandte gebiete*, **4**, 10–26.

Song, M. (2013). "Asymptotic theory for dynamic heterogeneous panels with cross-sectional dependence and its applications," manuscript, Columbia University.

Sparks, D.K., Khare, K., and Ghosh, M. (2015). "Necessary and sufficient conditions for high-dimensional posterior consistency under g-priors," *Bayesian Analysis*, **10**, 627–664.

van der Vaart, A. W. and Wellner, A. (1996). *Weak convergence and empirical processes*. Springer, New York.

Walker, S. G. and Hjort, N. L. (2001). "On Bayesian consistency," *Journal of the Royal Statistical Society*, **B63**, 811–821.

Yu, J., de Jong, R. and Lee, L-F (2008). "Quasi-maximum likelihood estimators for spatial dynamic panel data with fixed effects when both n and T are large," *Jounml of Econometrics*, **146**, 118–134.

Table 1: Banks included in the sample.

Ticker	Bank name	Total assets ($ in billions)	Total liabilities ($ in billions)	Total loans ($ in billions)	Total loans /assets (%)	Noninterest income/assets (%)
BAC	Bank of America	2,434	2,169	1,029	42.3	1.7
BARC*	Barclays US	149	132	41	27.3	4.4
BK	Bank of New York Mellon	382	340	55	14.3	3.5
C	Citigroup	1,951	1,757	718	36.8	1.3
CS*	Credit Suisse	115	92	13	11.0	5.1
DB*	Deutsche Bank USA	109	95	12	11.0	5.0
GS	Goldman Sachs Group	993	901	147	14.8	3.2
JPM	JPMorgan Chase Co.	2,688	2,426	993	37.0	2.2
MS	Morgan Stanley	895	813	173	19.3	3.9
STT	State Street Corporation	246	221	26	10.7	3.7
UBS*	UBS Americas	139	111	59	42.4	7.5
WFC	Wells Fargo	1,928	1,740	983	51.0	1.9

Note: Banks are listed in alphabetical order. Data source is from the publicly available FR Y-9C data, based on 2019Q4. The first three columns (total assets, total liabilities and total loans) are reported in $ billions and the last two columns (total loans as share of assets, noninterest income as share of assets) are both in percentage point. *indicates only U.S. subsidiaries of foreign-owned companies are reported.

Table 2: Total connectedness across quantiles (idiosyncratic shocks), pre-COVID vs COVID

quantile	pre-COVID	COVID
0.05	0.602	0.918
0.25	0.418	0.866
0.5	0.316	0.624
0.75	0.449	0.916
0.95	0.654	0.925

Note: Pre-COVID for 04/24/2017 - 12/31/2019; COVID for 01/01/2020 - 12/11/2020.
The interconnectedness measures are estimated based on all banks across time.

Table 3: Pairwise Directional Connectedness at group level (based on idiosyncratic shocks)

	pre-COVID				COVID		
quantile=0.05							
	Big4	Domestic	Foreign		Big4	Domestic	Foreign
Big4	0.37	0.33	0.30	Big4	0.34	0.57	0.10
Domestic	0.14	0.61	0.24	Domestic	0.33	0.56	0.11
Foreign	0.17	0.20	0.63	Foreign	0.35	0.57	0.09
quantile=0.25							
	Big4	Domestic	Foreign		Big4	Domestic	Foreign
Big4	0.51	0.24	0.25	Big4	0.56	0.35	0.09
Domestic	0.12	0.77	0.11	Domestic	0.58	0.38	0.04
Foreign	0.09	0.09	0.82	Foreign	0.43	0.34	0.23
quantile=0.5							
	Big4	Domestic	Foreign		Big4	Domestic	Foreign
Big4	0.66	0.18	0.16	Big4	0.37	0.30	0.33
Domestic	0.12	0.81	0.07	Domestic	0.17	0.53	0.30
Foreign	0.10	0.05	0.85	Foreign	0.11	0.19	0.69
quantile=0.75							
	Big4	Domestic	Foreign		Big4	Domestic	Foreign
Big4	0.58	0.16	0.26	Big4	0.61	0.16	0.23
Domestic	0.19	0.65	0.17	Domestic	0.51	0.30	0.19
Foreign	0.11	0.07	0.82	Foreign	0.45	0.25	0.30
quantile=0.95							
	Big4	Domestic	Foreign		Big4	Domestic	Foreign
Big4	0.47	0.23	0.30	Big4	0.74	0.20	0.05
Domestic	0.30	0.45	0.25	Domestic	0.70	0.23	0.07
Foreign	0.27	0.14	0.59	Foreign	0.71	0.23	0.06

Note: In this table, bank-level pairwise directional connectedness measures are at bank group level, averaged across banks within the group. Bank groups are defined as: Big4 banks (BAC, C, JPM, WFC), other domestic banks (BK, GS, MS, STT), and foreign banks (BARC, CS, DB, UBS). The left panel represents the pre-pandemic period and the right panel represents the pandemic period.

Table 4: To, From and Net measures at group level (based on idiosyncratic shocks)

	pre-COVID				COVID		
To							
quantile	Big4	Domestic	Foreign	quantile	Big4	Domestic	Foreign
0.05	0.50	0.65	0.65	0.05	0.93	1.56	0.27
0.25	0.38	0.49	0.39	0.25	1.42	0.96	0.21
0.5	0.39	0.30	0.26	0.5	0.43	0.70	0.74
0.75	0.54	0.31	0.50	0.75	1.44	0.65	0.66
0.95	0.83	0.51	0.62	0.95	2.00	0.61	0.16
From							
quantile	Big4	Domestic	Foreign	quantile	Big4	Domestic	Foreign
0.05	0.82	0.51	0.48	0.05	0.92	0.86	0.98
0.25	0.65	0.39	0.21	0.25	0.85	0.89	0.86
0.5	0.50	0.26	0.19	0.5	0.77	0.68	0.42
0.75	0.67	0.43	0.25	0.75	0.88	0.93	0.94
0.95	0.79	0.69	0.48	0.95	0.85	0.94	0.98
Net							
quantile	Big4	Domestic	Foreign	quantile	Big4	Domestic	Foreign
0.05	-0.31	0.14	0.17	0.05	0.01	0.70	-0.71
0.25	-0.28	0.11	0.17	0.25	0.57	0.07	-0.65
0.5	-0.11	0.04	0.08	0.5	-0.34	0.02	0.32
0.75	-0.13	-0.12	0.25	0.75	0.56	-0.28	-0.28
0.95	0.04	-0.18	0.14	0.95	1.15	-0.33	-0.82

Note: This table reports the three measures (To, From and Net) at bank group level, averaged across banks within the group. Bank groups are defined as: Big4 banks (BAC, C, JPM, WFC), other domestic banks (BK, GS, MS, STT), and foreign banks (BARC, CS, DB, UBS). The left panel represents the pre-pandemic period and the right panel represents the pandemic period.

Table 5: Quantile Connectedness, based on the Repo crisis during September 2019

	Based on idiosyncratic shocks			Based on common shocks			Based on both shocks		
Total Connectedness measure									
Total	0.929			0.875			0.916		
Pairwise Directional Connectedness									
	Big4	Domestic	Foreign	Big4	Domestic	Foreign	Big4	Domestic	Foreign
Big4	0.53	0.27	0.21	0.70	0.05	0.25	0.60	0.24	0.16
Domestic	0.42	0.35	0.23	0.58	0.08	0.34	0.49	0.30	0.21
Foreign	0.49	0.37	0.15	0.73	0.04	0.23	0.58	0.30	0.12
To, From and Net measures									
	Big4	Domestic	Foreign	Big4	Domestic	Foreign	Big4	Domestic	Foreign
To	1.36	0.85	0.54	1.77	0.13	0.73	1.61	0.73	0.45
From	0.93	0.86	0.96	0.76	0.97	0.90	0.94	0.88	0.96
Net	0.43	-0.01	-0.42	1.01	-0.84	-0.17	0.67	-0.16	-0.51

Note: This table reports the scenario-based quantile connecedness measures, during the Repo crisis in September 2019. The results contain three types of measures (from left panel to right panel): the connectedness measures based on idiosyncratic shocks, based on common shocks, and based on combined idiosyncratic and common shocks. For each type, we report the three main connectedness measures from top to bottom: total connectedness measure, pairwise directional connectedness measures (at group level), and finally the To, From and Net measures (at group level). Bank groups are defined as: Big4 banks (BAC, C, JPM, WFC), other domestic banks (BK, GS, MS, STT), and foreign banks (BARC, CS, DB, UBS).

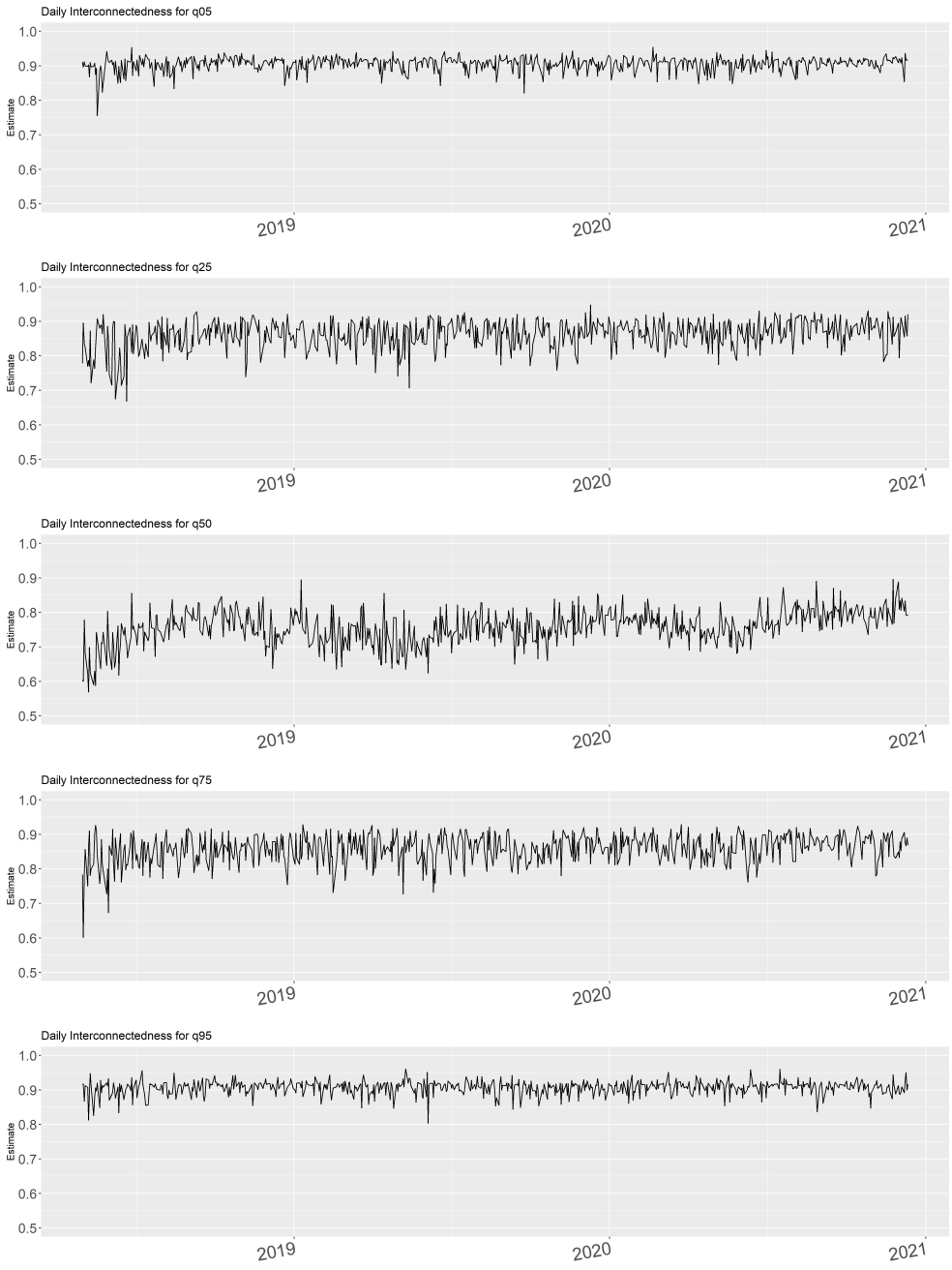

Figure 1: Time-varying total connectedness, across quantiles

Note: From top panel to bottom panel, quantile is 0.05, 0.25, 0.5, 0.75 and 0.95 respectively. The average and standard deviation of total connectedness are computed. The average total connectedness measures for quantiles $(0.05, 0.25, 0.5, 0.75, 0.95)$ are $(0.91, 0.86, 0.76, 0.86, 0.91)$ respectively. The corresponding standard deviations are $(0.02, 0.04, 0.05, 0.04, 0.02)$ respectively. The interconnectedness measures are estimated based on all banks across time.